JOURNAL
OF THE
WASHINGTON ACADEMY OF SCIENCES

VOL. 32 NOVEMBER 15, 1942 No. 11

CHEMISTRY.—*The third dissociation constant of phosphoric acid and its variation with salt content.*[1] ROGER C. WELLS.

In studying the origin of phosphate deposits W. W. Rubey, of the Geological Survey, found rather incomplete and conflicting information in the literature concerning the third dissociation constant of phosphoric acid, especially its variation with ionic strength. Such measurements as had been made covered chiefly very dilute solutions; some included the ionic strength of blood, but none that of sea water. At Mr. Rubey's request the writer has attempted to extend information on this subject, with the ultimate object of throwing light on the conditions under which phosphate deposits are supposed to be formed in nature.

The principal result of the investigation is that the concept of ionic strength is unnecessary and inapplicable. The constant appears to have values of a different order in salt solutions and in sea water from those obtaining when only phosphate buffers are present.

The constant desired was not the thermodynamic or activity constant but one generally termed the apparent dissociation constant, which has been found more useful for at least a first approach. The thermodynamic constant is based on the following equilibrium:

$$K_3 \times [HPO_4^{--}] = [H^+][PO_4^{---}] \quad (1)$$

in which the quantities in brackets represent the activities of the ions indicated. The first difficulty encountered is to determine these activities. As this has not yet been done for all conditions it is general practice to derive and use certain "apparent constants," which are suitable for practical work up to a certain point, and that practice is followed here. In this paper, then, $[PO_4^{---}]$ and $[HPO_4^{--}]$ are replaced by $[PO_4'''']$ and $[HPO_4'']$ meaning simply the stoichiometrical concentrations of those radicals, or, for example, such salts as trisodium phosphate and disodium phosphate, respectively. $[H^+]$ is retained with the usual significance of an ionic concentration; it was determined by hydrogen electrode measurements.

The apparent constant, K_3', although thus defined somewhat arbitrarily, shows a surprising constancy for widely different values of the concentration of the ions involved.

For ordinary practical purposes equation (1) shows that at any given pH the ratio $[PO_4'''']/[HPO_4'']$ must have a fixed value, or vice versa. Examined more minutely, however, the constant is found to vary slightly with temperature, with the concentration of the phosphate buffer salts and more particularly with the presence of other salts, such as sodium chloride or sea salts.

The constant is best determined by measuring $[H^+]$ in mixtures of, say, disodium phosphate and trisodium phosphate. These salts are of course not wholly ionized in moderate concentrations but they appear to be ionized to nearly the same extent, so that little is lost by using

$$\frac{[PO_4'''']}{[HPO_4'']} \quad \text{for} \quad \frac{[PO_4^{---}]}{[HPO_4^{--}]}.$$

Equilibrium (1) has little application to acid solutions because K_3 is very small and even a moderate quantity of hydrogen ions

[1] Published by permission of the Director, Geological Survey. Received July 15, 1942.

would convert practically all of the PO_4''' into HPO_4'' (or even into H_2PO_4'). It is only in alkaline solutions in which $[H^+]$ becomes small that $[PO_4''']$ becomes relatively large. Even for the alkalinity considered in this paper there must be a slight hydrolysis of the trisodium phosphate:

$$Na_3PO_4 + H_2O = NaOH + Na_2HPO_4. \quad (2)$$

This hydrolysis, the extent of which can be calculated from the pH, obviously results in a slight decrease in the Na_3PO_4 taken and an equal increase in the Na_2HPO_4 taken. This correction may be made a small one by using suitable proportions of the two phosphates.

As the solutions involved are sometimes made by neutralizing phosphoric acid with sodium hydroxide it is convenient to designate in some way the extent of the neutralization. This may be indicated by the letter R, ranging from 0 to 3. Thus 1 indicates that the neutralization has gone from 0 to 1, that is, from H_3PO_4 to NaH_2PO_4; 2 indicates Na_2HPO_4; and 3 indicates Na_3PO_4. Mixtures are intermediate. This number R has no reference to the total sodium in the solution but only to the amount of the hydrogen in the different phosphate combinations, H_3PO_4, H_2PO_4', HPO_4'', and PO_4'''. Thus, in sea water $[Na^+]$ is high but R would be about 2, indicating HPO_4^{--} as the principal phosphate ion. For most of the mixtures used in the present study R was 2.5. M_P is the total phosphate molality, so that for $R=2.50$ very nearly half of M_P is present as H_2PO_4'' and half as PO_4'''. This paper is largely a study of the pH of mixtures containing one mol of disodium phosphate to one mol of trisodium phosphate, with or without additional sodium chloride. M_{Cl} is the molality of chloride, generally NaCl, and M_S the total molality of sea salts. For average sea water with Cl = 1.900 per cent and density 1.027 $M_S = 0.514$.

The ionic strength, μ, is calculated as indicated by Lewis and Randall.[2]

PREVIOUS WORK

Nearly all previous work deals with relations in solutions containing only phosphate buffers. For some reason many results have been plotted against the ionic strength, but as the concept of ionic strength has been found of little use in the present investigation figures for it have been omitted in reviewing the previous work unless the authors used it exclusively.

Abbott and Bray[3] found 7.8×10^{-13} for K_3 at 0.05 M_P and 18° C., based on hydrolysis and conductivity measurements with ammonium salts. Making allowances for ionization they derived a figure of 3.6×10^{-13} for K_3 or 12.44 for pK_3 ($=-\log K_3$) but both values of K_3 are smaller than those calculated later from pH measurements by others using sodium salts.

From measurements by Salm[4] at 19° C., $M_P = 0.1$, and correcting for hydrolysis, one obtains the following results for K_3' and pK_3'.

R	$[PO_4''']$	$[HPO_4'']$
2.03	0.00293	0.097
2.14	0.0135	0.086

$[H^+]$	K_3'	pK_3'
9.8×10^{-11}	3.0×10^{-13}	11.52
1.3×10^{-11}	2.0×10^{-13}	11.47

Similar measurements by Ringer[5] were made at 18° C. from which I calculate $M_P = 0.0292$ and the following values of pK_3'.

R	$[PO_4''']$	$[HPO_4'']$	pH	pK_3
2.191	0.0048	0.024	10.97	11.66
2.66	0.0154	0.0136	11.77	11.72

Prideaux[6] gives data leading to the following figures ($M_P = 0.1$, t = 16° C.):

R	$[PO_4''']$	$[HPO_4'']$	pH	pK_3
2.05	0.0049	0.0950	10.23	11.52
2.10	0.0098	0.0902	10.60	11.57
2.16	0.0157	0.0843	10.70	11.43
2.19	0.0185	0.0815	10.89	11.54
2.22	0.0215	0.0785	10.92	11.48
2.50	0.0480	0.0520	11.54	11.57

E. Blanc[7] finds $pK_3' = 11.64$ at 25° C. for $M_P = 0.004$.

[2] LEWIS, G. N., and RANDALL, MERLE. *Thermodynamics*, p. 373, 1923.

[3] ABBOTT, G. A., and BRAY, W. C. Journ. Amer. Chem. Soc. 31: 760. 1909.

[4] SALM, E. Zeitschr. physikal. Chem. 57: 471. 1906.

[5] RINGER, W. E. Chemisch Weekblad 6: 446. 1909.

[6] PRIDEAUX, E. B. R. Journ. Chem. Soc. 99 (1): 1224. 1911.

[7] BLANC, E. Journ. Chim. Phys. 18: 28. 1920.

From Sörensen's measurements on Na_2HPO_4 Prideaux and Ward[8] calculate $pK_3' = 11.59$, based on $\frac{1}{15}$ M solutions.

Michaelis and Mizutani[9] find that $pK_3' = 11.53$ at 14° C. for $M_P = 0.02$ and that 60 per cent of alcohol raises this to 12.58, an effect which is in the opposite direction to that of sodium chloride studied in this paper.

Britton[10] finds $pK_3' = 11.57$ at 20° C. as an average over a range of R from 2.06 to 2.65 and M_P about 0.01, but without correction from the hydrolysis of PO_4'''.

Sendroy and Hastings[11] made a few determinations of pK_3' at 38° C. in solutions containing NaCl. Their figures decrease rapidly with increasing ionic strength, but they do not go above an ionic strength of 0.20.

Kugelmass[12] found 11.99 and 11.83 for pK_3' at 20° C. and 38° C. respectively for M_P ranging from 0.003 to 0.025. Little or no variation with the molality is indicated over the small range covered.

Bjerrum and Unmack[13] made measurements of potentials with very dilute sodium-phosphate solutions. Some of their results calculated as above give the following figures:

0°C.	R	$[PO_4''']$ (Corrected)	$[HPO_4'']$ (Corrected)	pH	pK_3'
18	2.333	0.01270	0.03020	11.39	11.77
18	2.500	0.01710	0.02290	11.64	11.77
18	2.333	0.00285	0.01002	11.37	11.92
25	2.333	0.01220	0.03070	11.28	11.68
25	2.500	0.01650	0.02350	11.50	11.66
25	2.333	0.00250	0.01030	11.20	11.82
37	2.333	0.01110	0.03180	11.07	11.52
37	2.500	0.01530	0.02470	11.28	11.48
37	2.333	0.00230	0.01050	10.92	11.59
Average pK_3' at 18° C. and $M_P = 0.042$					11.77
Average pK_3' at 25° C. and $M_P = 0.042$					11.67
Average pK_3' at 37° C. and $M_P = 0.042$					11.50

From the above results pK_3' appears to decrease with rising temperature at a given molality. The figures for lower molalities are apparently less reliable than the others. There is generally a decrease in pK_3' with increasing molality at each temperature.

Hahn and Klockmann[14] reach a figure of 11.89 for pK_3' in very concentrated solutions by means of a titration method.

Considering all the above measurements one may conclude that pK_3' decreases slightly with rising temperature and also with increasing molality. An average of five of the best results just referred to gives $pK_3' = 11.66$ at 20° C. and $M_P = 0.04$, whereas the writer finds 11.60.

METHODS

$[H^+]$ was determined by a hydrogen electrode combined with a tenth-normal calomel electrode. Liquid potentials were eliminated by making fresh connections with saturated potassium chloride before each measurement. A sodium-hydroxide solution was made by diluting a nearly saturated solution, as described by Sörensen, and protected from the carbon dioxide of the air. Mallinckrodt's $Na_2HPO_4 \cdot 12H_2O$ and H_3PO_4 were used. Some $Na_2HPO_4 \cdot 12H_2O$ was also recrystallized for this study by F. S. Grimaldi and used as the source of phosphate in most of the measurements. It was brought to the mixture $R = 2.50$ by adding sodium hydroxide. Dilutions were made with boiled freshly distilled water.

Definite mixtures were prepared, pH determined and $[H^+]$ calculated. From K_w $[OH^-]$ was calculated and taken as equal to the [NaOH] and $[Na_2HPO_4]$ formed by equation (2), from which the final $[HPO_4'']$ and $[PO_4''']$ were calculated. Values of K_w used were read from a curve passing through the following points:

[8] PRIDEAUX, E. B. R., and WARD, A. T. Journ. Chem. Soc. 125 (1): 423. 1924.

[9] MICHAELIS, L., and MIZUTANI, M. Zeitschr. physikal. Chem. 116: 135. 1925.

[10] BRITTON, H. T. S. Journ. Chem. Soc. 1927: 614.

[11] SENDROY, J., JR., and HASTINGS, A. B. Journ. Biol. Chem. 71: 783. 1927.

[12] KUGELMASS, I. N. Biochem. Journ. 23: 587. 1929.

[13] BJERRUM, N., and UNMACK, AUGUSTA. Danske Viden. Selskab., Math. fys. Med. 9: 1. 1929.

[14] HAHN, F. L., and KLOCKMANN, R. Zeitschr. physikal. Chem. 151: 80. 1930.

0° C.	0.11×10^{-14}
5	0.28×10^{-14}
10	0.28×10^{-14}
15	0.47×10^{-14}
20	0.72×10^{-14}
25	1.11×10^{-14}
30	1.70×10^{-14}
35	2.25×10^{-14}
40	2.80×10^{-14}

The variation of K_w with ionic strength was neglected, and only mixtures requiring a small correction for hydrolysis were considered, as dilute solutions and those involving a large correction for hydrolysis led to unreliable results. Moreover the variation of K_w with ionic strength is not known for higher ranges of the ionic strength.

RESULTS

The effect of temperature on the pH of phosphate mixtures is so small that it is difficult to detect with indicators. A "universal" indicator appeared to suggest a decrease in pH with rise of temperature, alizarin changed in the opposite direction, and malachite green faded out.

When determined by E.M.F. measurements the results for pH, with R between 2 and 3, showed a slight decrease with rise of temperature, in agreement with Bjerrum and Unmack. As K_w increases considerably with rising temperature the calculated values of K_3' in some instances decreased with rising temperature but in the great majority of instances K_3' increased with rising temperature. Facilities were not available to make measurements over a wide range of temperature. Based on results at 25° C. and 30° C. pH appeared to decrease about 0.02 unit per degree rise of temperature, agreeing fairly well with Bjerrum and Unmack, who found a decrease of 0.019 unit per degree. The calculations given in Table 5 for temperatures below 20° C. and above 30° C. are based on extrapolations on the latter basis.

The first series of measurements of pH and pK_3', shown in Table 1, was made with only the phosphate buffers, Na_3PO_4 and Na_2HPO_4, present. The combined molality of the two phosphate radicals is expressed as M_P.

The results presented in Table 1 show only a slight increase in pH with decreasing molality of the buffer mixtures, for all of which $R=2.50$. The change is approximately linear with $\sqrt{M_P}$, and may be represented by equation (3) at 27° C. The corresponding relation for pK_3' is given by equation (4).

$$\text{Buffer only.} \quad pH = 11.43 - 0.26\sqrt{M_P} \qquad (3)$$

$$\text{Buffer only.} \quad pK_3' = 11.57 - 0.50\sqrt{M_P} \qquad (4)$$

Similar equations hold for μ in place of M_P except that 0.26 and 0.50 become 0.13 and 0.25, respectively.

TABLE 1.—MEASUREMENTS OF pH AND pK_3' IN PHOSPHATE SOLUTIONS AT 27°, $R=2.50$

M_P	$\sqrt{M_P}$	pH	$K_3'\times10^{12}$	pK_3'
0.3014	0.550	11.28	5.21	11.28
0.2410	0.491	11.34	4.37	11.36
0.1929	0.440	11.29	4.86	11.31
0.1544	0.393	11.30	4.69	11.33
0.1205	0.347	11.32	4.36	11.36
0.0964	0.310	11.38	3.65	11.44
0.0771	0.278	11.37	3.63	11.44
0.0617	0.248	11.34	3.79	11.42
0.0493	0.222	11.39	3.14	11.50

If similar relations obtained when the ionic strength included sodium chloride the problem would be simple. Actually, the addition of sodium chloride introduces a shift of considerably greater magnitude, so that the results can no longer be represented simply as a function of the combined ionic strength, but they are rather some function of the ratio of foreign salt to the buffer phosphate salts. The use of the function ionic strength is, of course, not necessary in considering merely the effect of dilution on a single mixture of salts in a fixed proportion. A series of measurements is shown in Table 2 in which a buffered mixture containing

TABLE 2.—MEASUREMENTS OF pH AND pK_3' IN SOLUTIONS CONTAINING 3 MOLS OF PHOSPHATE TO 1 MOL OF SODIUM CHLORIDE 27° C., $R=2.50$

M_P	pH	$K_3'\times10^{12}$	pK_3'
0.1205	11.00	9.54	11.02
0.0964	11.05	8.41	11.08
0.0771	11.07	7.82	11.11
0.0617	11.13	6.61	11.18
0.0494	11.16	5.92	11.23
0.0395	11.18	5.38	11.27
0.0316	11.17	5.25	11.28

some sodium chloride was diluted over a considerable range.

Although the results for pH and pK_3' in Table 2 are linear with respect to $\sqrt{M_P}$ they are all considerably lower than corresponding results in Table 1 and they do not extrapolate to the same figure for $\sqrt{M_P}=0$. On the other hand, if P and NaCl are varied independently irregular results are obtained. Furthermore, the lowering effect of NaCl can not be expressed as any simple function of the combined ionic strength.

As the outcome of numerous trials the following equations (5) and (6) for pH and pK_3' respectively were found to take account of various mixtures of buffer ($R=2.50$) and NaCl at 27° C. fairly well. Their application is shown in Table 3.

In salt solutions.

$$pH = 11.43 - 0.26\sqrt{M_P} - 0.98\sqrt[3]{M_{NaCl}} \quad (5)$$

In salt solutions.

$$pK_3' = 11.57 - 0.50\sqrt{M_P} - 0.98\sqrt[3]{M_{NaCl}} \quad (6)$$

Inasmuch as the ionic strength does not apply in general it is impossible to give an equation based on ionic strength without considering the nature of the salts.

In sea water pH is controlled largely by carbonates, R for the phosphates in sea water is much below 2.50, and the question arose whether equation (6) would be applicable. Some experiments with artificial sea water showed that the effect of sea salts is very similar to that of sodium chloride and that M_S can be used for M_{NaCl} in equations (5) and (6).

When sea salts are added to the phosphate buffers a precipitate of calcium phosphate is thrown down. A solution, however, was made up containing all the principal constituents of sea water except calcium and magnesium but with 0.054 mol of potassium chloride per liter and 0.010 mol per liter of the phosphate buffers substituted for the calcium and magnesium salts and sodium bicarbonate. The composition of representative sea water and that of the imitation sea water are shown in Table 4.

TABLE 4.—NORMAL SEA WATER AND IMITATION SEA WATER. MOLS PER LITER

Constituent	Normal	Imitation
NaCl	0.412	0.412
$MgCl_2$	0.052	None
Na_2SO_4	0.028	0.028
$CaCl_2$	0.010	None
KCl	0.009	0.063
$NaHCO_3$	0.002	None
KBr	0.001	0.001
Phosphate	—	0.010
Total	0.514	0.514

The results for pH and pK_3' obtained with the imitation sea water are included in Table 3, next to the last row. They show that equations (5) and (6) are applicable if M_S is used in place of M_{NaCl} where S is the total molality of the sea salts. The last row gives results when this sea water was diluted one half; although they are not so good they are of the right order and confirm the applicability of equations (5) and (6).

In any equation for pK_3' for sea water M_P is really negligible, so that, as a result

TABLE 3.—EFFECT OF NaCl AND SEA SALTS ON pH AND pK_3' OF PHOSPHATE SOLUTIONS. 27° C., $R=2.50$

M_P	M_{NaCl}	$\sqrt{M_P}$	$\sqrt[3]{M_{NaCl}}$	pH observed	pH calc. by (5)	pK_3' observed	pK_3' calc. by (6)
0.0100	0.0100	0.100	0.215	11.13	11.19	11.46	11.31
0.0100	0.1000	0.100	0.464	11.00	10.95	11.23	11.07
0.0100	0.5333	0.100	0.811	10.57	10.61	10.66	10.73
0.0100	1.0000	0.100	1.000	10.38	10.42	10.45	10.54
0.0150	0.8000	0.122	0.929	10.57	10.49	10.51	10.60
0.0316	0.0105	0.178	0.219	11.17	11.17	11.28	11.28
0.0493	None	0.222	—	11.39	11.37	11.50	11.46
0.0100	0.513[a]	0.100	0.800[a]	10.64	10.62[a]	10.74	10.74[a]
0.0050	0.256[a]	0.071	0.634[a]	10.59	10.79[a]	10.77	10.91[a]

[a] Using M_S (molality of sea salts) instead of M_{NaCl}.

of the above experiments and calculations, we may write the following tentative equation for sea water at 27° C.:

$$pK_3' = 11.57 - 0.98\sqrt[3]{M_S} \qquad (7)$$

Although equations (5), (6), and (7) are empirical, they seem to be a great improvement over extrapolations of equations that have been suggested previously. In studying the second dissociation constant of phosphoric acid J. W. H. Lugg[15] gives an equation of the following form to represent the relations when the ionic strength is contributed almost entirely by a foreign salt like sodium chloride:

$$pK' = pK - \frac{1.5}{1+n} \qquad (8)$$

in which n ranges from 0.60 for NaCl to 1.65 for the buffers alone. Such an equation may be applicable to the third dissociation constant in the presence of any given single salt, but it is not known whether it could be applied to mixtures like sea water.

Table 5 presents rounded values of pK_3' calculated for the conditions stated. Other values may be computed by equations (4), (6), or (7), taking account of variation with temperature, or interpolated from those given in the table. M_X represents M_P when only buffers are present and either M_{NaCl} or M_S when sodium chloride or sea salts are in considerable excess.

The variation of pK_3' with the molality of the phosphate and sodium chloride, respectively, at 27° C. is shown in Fig. 1. The lower curve refers to the buffer mixtures, the upper to a large excess of sodium chloride or sea water. The lines are based on results calculated from the equations; the experimental results suggest a very slight curvature instead of straight lines.

The interest and assistance of W. W. Rubey, P. G. Nutting, F. S. Grimaldi, K. J. Murata, and H. C. Spicer in the preparation of this paper are gratefully acknowledged. Mr. Rubey especially contributed many helpful suggestions and verified the calculations.

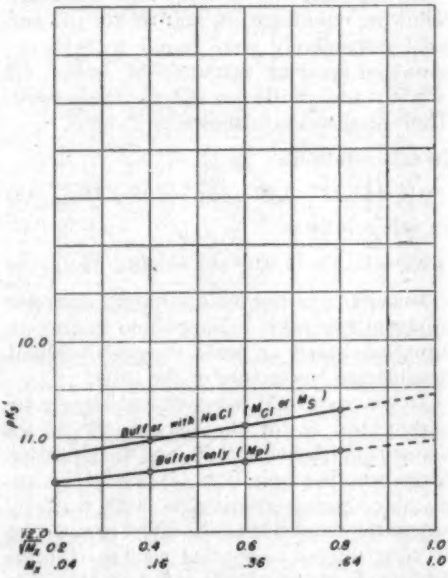

Fig. 1.—Variation of pK_3' with molality at 27° C. Lower curve, buffer mixture; upper curve, a large excess of NaCl or sea water.

[15] Trans. Faraday Soc. 27: 297. 1931.

TABLE 5.—VALUES OF pK_3' AT CERTAIN TEMPERATURES AND MOLALITIES (M)

	M_X =	0.04	0.16	0.36	0.64
In presence of only buffer of strength indicated	Temp. 0° C.	11.98	11.88	11.78	11.68
	10°	11.79	11.69	11.59	11.49
	20°	11.60	11.50	11.40	11.30
	30°	11.41	11.31	11.21	11.11
	40°	11.22	11.12	11.02	10.92
In presence of a large excess of NaCl or sea salts of strength indicated	0°	11.74	11.55	11.39	11.24
	10°	11.55	11.36	11.20	11.05
	20°	11.36	11.17	11.01	10.86
	30°	11.17	10.98	10.82	10.67
	40°	10.98	10.79	10.63	10.48

CRYSTALLOGRAPHY.—*Morphologie de l'idocrase.*[1] Abbé J.-ARTHUR TREMBLAY, Université Laval, Québec (Canada). (Communicated by G. TUNELL.)

SOMMAIRE

Étude détaillée de l'importance relative des formes cristallines de l'idocrase, $Ca_{10}Mg_2Al_4Si_9O_{34}(OH)_4$. Le groupe spatial s'en déduit par la méthode morphologique de Donnay (1939). On trouve *C4/acn*, avec le rapport d'axes habituel $c:a=0.5372$. En tournant le cristal de 45°, le rapport d'axes devient $c:a=0.7597$, et le groupe s'écrit *P4/nnc*. Le groupe spatial trouvé au moyen des rayons X (*Strukturbericht*, **2**: 127, 1937) est bien *P4/nnc*.

L'ordre observé d'importance relative des formes est comparé à l'ordre théorique, dans le cas de la loi de Bravais classique, qui donnait l'aspect *I****, et dans le cas de la loi généralisée (Donnay et Harker, 1937), qui conduit au groupe *P4/nnc*. L'accord est meilleur dans ce dernier cas, quoique certaines anomalies persistent.

INTRODUCTION

L'analyse morphologique des espèces cristallines par la méthode Donnay (1939) conduit au groupe spatial, sans nécessiter l'emploi des rayons X. L'importance relative des formes extérieures reflète la symétrie interne, c'est-à-dire celle de la disposition des atomes à l'intérieur de la maille. Tel est le point de départ de cette méthode, d'après laquelle sept minéraux, jusqu'à présent, ont été étudiés de façon détaillée. Donnay a publié des travaux sur cinq d'entre eux: l'apophyllite, tétragonale (1937); le rutile et le zircon, tétragonaux (1938a); la danburite, orthorhombique (1940b); la microlite, isométrique (1941). Les deux autres, la columbite et la stéphanite, orthorhombiques, ont été traités par un de ses élèves, E. D. Taylor (1940a et b). Le groupe spatial trouvé est, dans chaque cas, celui qu'ont donné les rayons X, sauf pour la columbite, où le développement de la zone des faces (0*kl*) s'avère incompatible avec les résultats radiologiques.

On trouvera dans ce travail l'application de la méthode au cas de l'idocrase (ou vésuvienne). Plusieurs formules ont été proposées pour ce minéral. *Strukturbericht* (**2**: 127. 1937) donne celle de C. Gottfried, $Ca_{10}Mg_2Al_4Si_9O_{34}(OH)_4$.

L'idocrase cristallise dans le système tétragonal. Elle présente le plus souvent un facies prismatique allongé, avec tantôt le prisme *m* {110} dominant, tantôt le prisme *a* {010}. Elle montre assez fréquemment un facies pyramidal et très rarement le facies tabulaire basal (Fig. 1.)

DONNEES D'OBSERVATION

L'*Atlas der Krystallformen* de Goldschmidt (1918) reproduit 249 cristaux d'idocrase. De ces figures, sept sont illisibles et quinze autres représentent des cristaux de localité inconnue. Négligeant ces 22 figures, il en reste 227 dont l'étude statistique montrera la fréquence et le développement des formes représentées. Sur ces figures apparaissent 47 formes, que je désignerai par les lettres conventionnelles de Goldschmidt. L'orientation habituelle ($c:a=0.5372$) sera provisoirement utilisée. On ne tiendra aucun compte du clivage pour décider de l'importance des formes (Donnay, 1938a). L'importance d'une forme relève en tout premier lieu de sa fréquence; la grandeur des faces n'intervient que pour départager des formes d'à peu près même fréquence.

L'étude statistique est menée comme suit.

(1) On examine d'abord toutes les figures d'une même localité. Pour chacune de ces figures, on fait le relevé des formes par ordre de grandeur décroissante (voir tableau 1, pour le cas des cristaux de Pfitsch).

TABLEAU 1.—PFITSCH (TYROL)

N° de la fig.	Observateur	Classement des formes
133	Zepharovich	*p a ϑ m c f (i s) t*
134	Zepharovich	*a m p f ϑ i s c t*
135	Zepharovich	*p a m ϑ c f o h (i d) (s b) t x u*
136	Zepharovich	*p ϑ c m i b t s d u*
137	Zepharovich	*m p c i s o μ*
156	Groth	*a m f p c s ϑ i d b o t u e*

[1] Received May 15, 1942.

On en tire la *fréquence* de chaque forme pour la localité considérée, c'est-à-dire le nombre de fois que la forme a été représentée. On calcule ensuite le *rang moyen* de chaque forme de la façon suivante (voir tableau 2, pour le cas des cristaux du Vésuve): en face de chaque forme, désignée par la lettre de Goldschmidt et les indices de Miller, on indique combien de fois elle occupe le 1er rang, le 2e rang, . . . etc. Dans l'exemple du Vésuve, la forme *a* {010}, sur 35 cristaux figurés, vient 16 fois au 1er rang, 9 fois au 2e, 6 fois au 3e, 4 fois au 4e; son rang moyen est $(16\times1+9\times2+6\times3+4\times4)/35=1.9$. Le rang moyen donne donc une mesure approximative de la grandeur, laquelle est d'autant plus considérable que le rang moyen est plus petit. Le résultat est une liste de formes classées par ordre d'importance pour la localité étudiée (les formes d'importance à peu près égale sont réunies entre parenthèses).

Trois tableaux sont donnés à titre d'exemples: Vésuve, facies prismatique avec *a* dominant (tableau 2); Piémont, facies prismatique avec *m* dominant (tableau 3); Pfitsch (Tyrol), facies pyramidal avec *p* dominant (tableau 4).

(2) On examine ensuite les différents classements obtenus pour les diverses localités (tableau 5). On en tire la *fréquence absolue* ou fréquence de localité, c'est-à-dire le nombre de localités où la forme est représentée. On calcule ensuite son *rang moyen de localité* (comme ci-dessus pour le rang moyen de figure). On arrive ainsi (tableau 6) à dresser la liste finale[2] des formes par

[2] Pour obtenir le rang moyen de localité, on peut accorder plus de poids aux localités qui sont représentées par un nombre plus grand de figures. Le résultat est alors le suivant: *m a* (*c p*) *s f t o i ϑ h b z u x d r v γ ω η n* (*α π*) *ν β ξ* (*ψ Δ*) *e l δ σ q y φ g F* Y_2 L_1 L_2 Y_3 (*ε* r_1) ?*N* *μ λ*. On voit que cette liste ne diffère guère de celle du tableau 6, surtout en ce qui concerne les formes les plus importantes.

TABLEAU 2.—VÉSUVE (FACIES PRISMATIQUE, *a* DOMINANT)

Nombre de cristaux figurés: 35 Nombre total de formes figurées: 30
Nombre de formes par cristal: minimum, 4; maximum, 18.

Lettre	Formes Indices	Fréquence	Nombre de figures où la forme occupe le rang suivant:																	Rang moyen
			1er	2e	3e	4e	5e	6e	7e	8e	9e	10e	11e	12e	13e	14e	15e	16e	17e	18e	
a	010	35	16	9	6	4	..	..	..	..	..	..	..	..	..	..	..	..	..	..	1.9
m	110	35	13	10	6	3	1	2	..	..	..	..	..	..	..	..	..	..	..	..	2.3
p	111	35	3	10	14	5	2	..	1	..	..	..	..	..	..	..	..	..	..	..	2.9
c	001	35	5	5	5	12	6	1	1	..	..	..	..	..	..	..	..	..	..	..	3.4
f	120	27	..	..	9	8	5	2	1	..	1	..	..	..	1	..	..	..	..	..	4.6
o	011	25	..	..	1	2	4	6	4	6	..	..	..	..	1	1	..	..	..	..	6.8
i	132	20	..	1	..	..	2	3	2	1	2	2	3	2	1	1	..	..	..	..	8.7
s	131	16	..	..	..	..	2	2	2	5	1	3	..	1	..	..	..	..	..	..	7.9
ϑ	113	15	..	..	..	..	1	4	3	2	1	2	1	1	..	..	..	..	..	..	7.9
t	331	11	..	..	..	..	2	2	3	..	3	1	..	..	..	..	..	..	..	..	7.3
h	130	9	..	..	..	2	4	1	..	1	..	..	1	..	..	..	..	..	..	..	5.9
z	121	8	..	..	..	..	..	1	1	1	2	3	..	..	..	..	..	..	..	..	8.6
b	221	4	..	..	..	..	1	1	1	..	..	..	..	..	1	..	..	..	..	..	7.7
d	241	4	..	..	..	..	..	1	..	1	2	..	..	..	..	..	..	..	..	..	8.0
y	141	4	..	..	..	..	..	..	..	..	2	..	1	..	1	..	..	..	..	..	10.5
v	151	4	..	..	..	..	..	..	..	..	1	1	1	1	..	..	..	..	..	..	10.5
ξ	032	3	..	..	..	..	..	..	..	..	2	1	..	..	..	..	..	..	..	..	9.3
r	112	3	..	..	..	..	..	..	..	..	1	2	..	..	..	..	..	..	..	..	9.6
u	021	3	..	..	..	..	..	1	..	..	..	1	..	..	1	..	..	..	..	..	9.6
l	243	2	..	..	..	..	..	1	..	1	..	..	..	..	..	..	..	..	..	..	7.0
π	031	2	..	..	..	..	..	..	..	1	1	..	..	..	..	..	..	..	..	..	8.5
ω	377	..	..	..	..	..	..	..	..	..	..	..	..	..	..	..	..	..	..	..	6.0
g	5.20.2	..	..	..	..	..	..	..	..	..	..	..	..	..	..	..	..	..	..	..	7.0
ν	012	..	..	..	..	..	..	..	..	..	..	..	..	..	..	..	..	..	..	..	11.0
F	7.13.1	..	..	..	..	..	..	..	..	..	..	..	..	..	..	..	..	..	..	..	12.0
x	133	..	..	..	..	..	..	..	..	..	..	..	..	..	..	..	..	..	..	..	12.0
Y_2	481	..	..	..	..	..	..	..	..	..	..	..	..	..	..	..	..	..	..	..	13.0
L_1	8.10.15	..	..	..	..	..	..	..	..	..	..	..	..	..	..	..	..	..	..	..	14.0
L_2	371	..	..	..	..	..	..	..	..	..	..	..	..	..	..	..	..	..	..	..	15.0
Y_3	5.19.2	..	..	..	..	..	..	..	..	..	..	..	..	..	..	..	..	..	..	..	16.0

Classement définitif: *a m p c f o i* (*ε ϑ*) (*t h*) *z b d* (*y v*) *ξ r u*) *l π ω g ν* F *x* Y_2 L_1 L_2 Y_3.

ordre d'importance décroissante, pour l'espèce.

PROJECTION GNOMONIQUE

On adopte l'ordre d'importance décroissante des formes trouvé au tableau 6, savoir:

m	*a*	(*c*	*p*)	*s*	*f*	(*t*	*o*)	*i*	*ϑ*
110	010	001	111	131	120	331	011	132	113
h	*u*	(*z*	*b*)	*d*	*r*	*x*	*v*	*γ*	*η*
130	021	121	221	241	112	133	151	118	114
α	*n*	*π*	*ν*	*ω*	*l*	Δ	*ψ*	*e*	
1.1.20	122	031	012	377	243	454	470	351	
(*σ*	*δ*)	*β*	*ξ*	(*ε*	*q*	λ)	r_1	*μ*	
135	117	1.1.10	032	116	383	445	461	885	
y	*φ*	?N	*g*	F	Y_2	L_1	L_2		
141	350	441	5.20.2	7.13.1	481	8.10.5	571		
Y_3									
5.19.2									

Outre ces 47 formes, relevées sur les dessins de l'*Atlas* de Goldschmidt, il en existe beaucoup d'autres qui, bien qu'ayant été observées, n'ont jamais été figurées.

L'ordre de ces formes est mis en évidence sur la projection (Fig. 2): les pôles gnomoniques sont marqués par des cercles dont le rayon décroît avec l'importance de la forme correspondante. La symétrie tétragonale holoèdre permet d'utiliser seulement la moitié d'un octant, l'octant avant-droit-supérieur, où tous les indices sont positifs. La projection gnomonique est ici un carré coupé par une diagonale. C'est la partie située au-dessus de la diagonale qui est employée dans l'étude des zones et dans la recherche du groupe spatial. Comme le groupe trouvé imposera un changement d'orientation, la partie de la projection située au-dessous de la diagonale montre la projection gnomonique du cristal dans la nouvelle orientation. Pour cela, on n'a qu'à tourner la feuille de 45°, dans le sens contraire à celui de la marche des aiguilles d'une montre. L'étude comparative des deux orientations met en évidence la différence de grandeur des deux mailles, les changements d'indices des faces et la variation du type des zones.

DETERMINATION DU MODE DU RESEAU ET DE LA FACE UNITAIRE

On détermine le mode du réseau en se basant sur l'étude des zones dont les faces ne sont perpendiculaires à aucun plan de symétrie. Dans la zone des faces (*hkh*) on

TABLEAU 3.—ALPE MUSSA, PIÉMONT (FACIES PRISMATIQUE, *m* DOMINANT)

Nombre de cristaux figurés: 36
Nombre total de formes figurées: 20
Nombre de formes par cristal: minimum, 2; maximum, 11

Lettre	Formes Indices	Fréquence	Nombre de figures où la forme occupe le rang suivant												Rang moyen
			1er	2e	3e	4e	5e	6e	7e	8e	9e	10e	11e	12e	13e	
m	110	36	30	3	3	..	..	..	..	..	..	..	..	..	..	1.3
a	010	34	5	20	8	..	..	1	..	..	..	..	..	..	..	2.2
c	001	32	..	8	9	5	5	2	3	..	..	..	..	..	..	3.8
p	111	32	..	1	9	13	4	3	2	..	..	..	..	..	..	4.2
s	131	29	..	1	2	5	8	3	5	3	2	..	..	..	..	5.6
t	331	22	..	1	..	2	2	9	4	3	1	..	..	..	..	6.0
o	011	16	..	..	..	4	6	3	..	2	1	..	..	..	..	5.6
i	132	15	..	..	1	..	2	5	4	3	..	..	..	..	..	6.3
f	120	10	1	1	2	4	2	..	..	..	..	..	..	..	..	3.5
ϑ	113	9	..	..	..	..	..	..	3	..	4	1	1	..	..	8.7
b	221	3	..	..	..	..	..	1	1	..	1	..	..	..	..	7.3
q	383	2	..	..	..	..	..	..	..	2	..	..	..	..	..	8.0
γ	118	2	..	..	..	..	..	..	..	1	..	1	..	..	..	9.0
β	1.1.10	2	..	..	..	..	..	..	..	1	..	1	..	..	..	9.0
z	121	2	..	..	..	..	..	..	..	1	..	..	1	..	..	9.5
ψ	470	..	..	1	..	..	..	..	..	..	..	..	..	..	..	2.0
φ	350	..	..	1	..	..	..	..	..	..	..	..	..	..	..	2.0
α	1.1.20	..	..	..	..	..	..	..	..	..	1	..	..	..	..	9.0
δ	117	..	..	..	..	..	..	..	..	..	..	1	..	..	..	10.0
σ	135	..	..	..	..	..	..	..	..	..	..	..	1	..	..	11.0

Classement définitif: *m a* (*c p*) *s t o i f ϑ b q* (*γ β*) *z* (*ψ φ*) *α δ σ*.

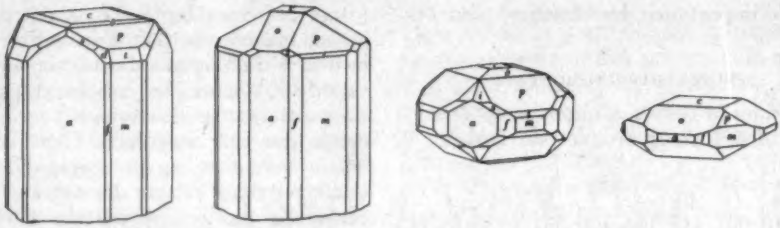

Fig. 1.—Différents facies de l'idocrase: prismatique allongé avec *a* (Vésuve) ou *m* (Piémont) dominant, pyramidal trapu (Tyrol) et tabulaire épais (Laurel, Argenteuil, Québec).

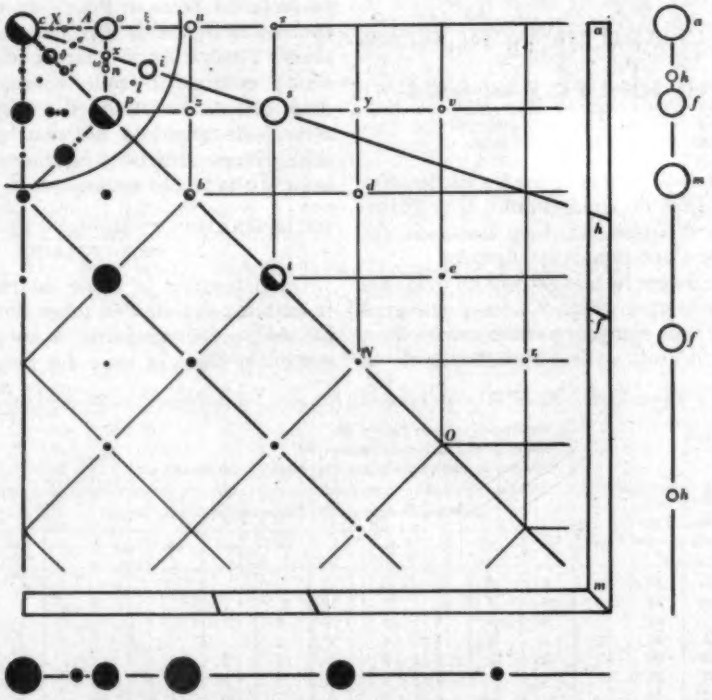

Fig. 2.—Projection gnomonique de l'idocrase (octant avant-droit-supérieur). Au-dessus de la diagonale, orientation *C;* en-dessous, orientation *P*.

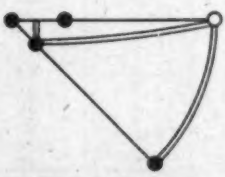

Fig. 3.—Aspect C^{***}

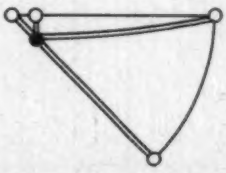

Fig. 4.—Aspect $C4/acn$

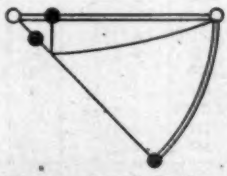

Fig. 5.—Aspect $P4/nnc$

Tableau 4.—Pfitsch (Tyrol) (Facies Pyramidal)

Nombre de cristaux figurés: 6 Nombre total de formes figurées: 16
Nombre de formes par cristal: minimum, 7; maximum, 15

Lettre	Formes Indices	Fréquence	Nombre de figures où la forme occupe le rang suivant:														Rang moyen
			1er	2e	3e	4e	5e	6e	7e	8e	9e	10e	11e	12e	13e	14e	15e	
p	111	6	3	1	1	1	..	..	..	..	..	..	..	..	..	..	..	2.0
m	110	6	1	2	1	2	..	..	..	..	..	..	..	..	..	..	..	2.6
c	001	6	..	..	2	..	3	..	..	1	..	..	..	..	..	..	..	4.8
i	132	6	..	..	..	1	..	2	1	1	1	..	..	..	..	..	..	6.6
ϑ	113	5	..	1	1	1	1	..	1	..	..	..	..	..	..	..	..	4.2
a	010	4	2	2	..	..	..	..	..	..	..	..	..	..	..	..	..	1.5
s	131	5	..	..	..	..	1	..	2	1	..	..	1	..	..	..	..	7.6
t	331	5	..	..	..	..	..	1	..	2	..	..	1	1	..	..	..	9.0
f	120	4	..	..	1	1	..	2	..	..	..	..	..	..	..	..	..	4.8
o	011	3	..	..	..	..	..	1	1	..	..	..	1	..	..	..	..	7.6
b	221	3	..	..	..	..	..	1	..	..	..	1	1	..	..	..	..	9.0
d	241	3	..	..	..	..	..	..	..	..	3	..	..	..	..	..	..	9.0
u	021	3	..	..	..	..	..	..	..	..	..	1	..	..	1	..	1	12.6
μ	885	..	..	..	..	..	..	..	1	..	..	..	..	..	..	..	..	7.0
x	133	..	..	..	..	..	..	..	..	..	..	..	..	..	..	1	..	14.0
e	351	..	..	..	..	..	..	..	..	..	..	..	..	..	..	1	..	14.0

Classement définitif: *p m c (i ϑ a) s (t f) o b d u μ (x e).*

Tableau 5.—Classement des Formes dans les Diverses Localités (47 Formes—227 Figures—37 Localités)

Localité	Classement des formes	A	B	C	D
1. Alpe Mussa (Piémont)	*m a (c p) s t o i f ϑ b q (γ β) z (ψ φ) α δ σ*	36	20	2	11
2. Vésuve	*a m p e f o i (s ϑ) (t h) z b d (y v) ξ (r u) l π ω g ρ* F *x* Y_3 L_3 L_1 Y_1	35	30	4	18
3. Wilui (Sibérie)	*(m p) c a o t i s f u ϑ b z*	17	11	4	8
4. Monte Somma (Vésuve)	*m a c p f o s r i b ϑ u h x π η (v l)* ?N *ϑ α d (z ξ β ω n)*	14	27	4	17
5. Zermatt (Suisse)	*m a c (z p) ϑ (i t) o ω f e b x e n*	13	16	4	14
6. Piémont	*m a (c p) s o f t i ϑ h*	11	11	3	9
7. Val de Susa (Italie)	*a (c m) p o t z f i s (d Δ)*	11	12	5	9
8. Aberdeenshire (Ecosse)	*m p c a f t s r h o η u r_1 γ i z x*	10	17	5	10
9. Autres localités (Norvège)	*a m (o c) h ϑ p f i e u v (η φ) γ*	8	15	3	11
10. Oural	*a m p (s t c) i n s o r*	7	11	5	10
11. Pfitsch (Tyrol)	*p m c (i ϑ a) s (t f) o b d u μ (x e)*	6	16	7	15
12. Eker (Norvège)	*m c (f a) p e ϑ i h v r i γ*	6	13	6	11
13. Tennberget (Dalarne)	*m c a p o t s f u h d i*	5	12	5	12
14. Monzoni (Val de Fassa) (Tyrol)	*(a m) p c t o b (f e)*	4	9	6	7
15. Aarvold (Norvège)	*p c m (f o a) t s*	4	8	1	7
16. Monti Albani (Italie)	*(a m p) c t o f s h ϑ v s u d i*	4	5	5	15
17. Nelle-Galles du Sud	*m a p s t (c o i)*	3	8	5	8
18. Ala (Piémont)	*a m c t e p h z o f b i ϑ*	3	13	3	8
19. Csiklova (Hongrie)	*p m a o c*	3	5	3	4
20. Combe Robert, Avigliana (Piémont)	*m a c p s t i o s*	2	9	8	9
21. Frugard (Suède)	*a c m*	2	3	3	3
22. Finlande	*c m e f h*	2	5	4	5
23. Nombreuses localités	*m (p a) h o s ϑ r*	2	8	4	8
24. Egg (Norvège)	*(m a) c p (f i) α*	2	7	5	6
25. Pyrénées	*a m p c o f s*	2	7	3	7
26. Friedsberg (Silésie)	*m (c a) p z (h o) ϑ d i r u*	2	12	4	11
27. Predazzo (Tyrol)	*m (a p) f o c s i t (ϑ z) λ b ω δ*	2	15	10	13
28. Vallée de Saas (Valais)	*m a s t*	2	4	4	4
29. Gross-Venediger (Tyrol)	*m p z f (ϑ l) c e u i*	1	10		
30. Sandford, Me (U.S.A.)	*m a c f h i p u e d t r*	1	12		
31. Pajsberg (Suède)	*a m p f c o s i*	1	8		
32. Kiura (Prov. Bungo)	*m a f p c l ϑ o i*	1	9		
33. Cintra (Portugal)	*(m a) (f p) c i s*	1	7		
34. Manesteock (Groenland)	*c a m f p i*	1	6		
35. Gweedore in Donegal (Irlande)	*m c (a f) o*	1	5		
36. Amity (Orange City)	*m p*	1	2		
37. Raon l'Etape (Vosges)	*m a c i p*	1	5		

A: nombre de cristaux figurés pour la localité considérée.
B: nombre de formes figurées pour la localité considérée.
C: nombre minimum de formes figurées sur un cristal.
D: nombre maximum de formes figurées sur un cristal.

observe (tableau 8): $p\ s\ z\ v\ y\ \Delta\ q$. Le *segment arithmétique*[3] donne s à la distance 3, z à 4/2, v à 5, y à 8/2 (op étant pris pour unité). A cause de la symétrie tétragonale holoèdre, cette zone est la même que celle des (hkk), qui contient les faces du *segment harmonique*[3]: $x\ n\ \omega$. La face x est à la distance 1/3, n à 2/4, et ω à 3/7. On a évidemment affaire à une zone double avec dominante unitaire simple p. Cette zone ne suffit pas, à elle seule, pour déterminer la mode du réseau. Elle élimine le mode primitif (P) et le mode à maille centrée (I), montrant qu'on est dans l'autre orientation. Reste à voir si le réseau est à base centrée (C) ou à faces centrées (F).

Les renseignements nécessaires seront fournis par l'étude d'une autre zone, dont le type sera différent dans les deux modes. L'équation de la zone $c\ i\ s$ est $k=3h$. Toutes les faces de cette zone satisfont donc au critère $\mathbf{C}=(h+k)$ pair, et la zone doit être du type simple, avec (131) dominante, dans le cas d'un réseau C. Par contre, dans le cas d'un réseau F, la zone deviendrait double, avec la même dominante. Or, la zone $c\ i\ s$ comprend les faces $s\ i\ x\ \sigma$, qui sont respectivement aux distances 1, 1/2, 1/3, 1/5 (tableau 7). C'est donc une zone simple, et le réseau est C. On relève une anomalie dans le manque de face à la distance 1/4, mais σ (à la distance 1/5) n'est signalée que deux fois dans les figures de l'*Atlas*. Les trois autres faces, beaucoup plus importantes, ne laissent aucun doute sur le type, simple, de cette zone (i est nettement plus importante que x). Puisque la dominante s doit s'écrire (131), on en déduit que p est bien la face unitaire (111).

[3] La terminologie employée ici est celle de la *règle harmonique-arithmétique*, due à Peacock (1936).

DETERMINATION DU GROUPE SPATIAL

Les zones dont les faces sont perpendiculaires à un plan de symétrie, miroir ou plan avec glissement, serviront à déterminer le groupe spatial. Ce sont les zones des faces

TABLEAU 6.—CLASSEMENT DÉFINITIF DES FORMES

Formes			Nombre de localités où la forme occupe le rang suivant:																												Rang moyen
Lettre	Indices	Fréquence absolue	1er	2e	3e	4e	5e	6e	7e	8e	9e	10e	11e	12e	13e	14e	15e	16e	17e	18e	19e	20e	21e	22e	23e	24e	25e	26e	27e	28e	29e	30e	
m	110	37	24	10	3	..	..	..	..	..	..	..	..	..	..	..	..	..	..	..	..	..	..	..	..	..	..	..	..	..	..	..	1.4
a	010	36	13	13	6	4	..	..	..	..	..	..	..	..	..	..	..	..	..	..	..	..	..	..	..	..	..	..	..	..	..	..	2.0
c	001	34	2	7	12	6	4	2	1	..	..	..	..	..	..	..	..	..	..	..	..	..	..	..	..	..	..	..	..	..	..	..	3.4
p	111	33	5	5	9	8	3	1	2	..	..	..	..	..	..	..	..	..	..	..	..	..	..	..	..	..	..	..	..	..	..	..	3.3
s	131	28	..	..	1	3	6	2	8	6	1	1	..	..	..	..	..	..	..	..	..	..	..	..	..	..	..	..	..	..	..	..	6.4
f	120	27	..	..	4	7	4	1	2	4	3	1	1	..	..	..	..	..	..	..	..	..	..	..	..	..	..	..	..	..	..	..	5.9
t	331	26	..	..	..	4	5	7	2	3	1	1	1	1	..	..	..	..	1	..	..	..	..	..	..	..	..	..	..	..	..	..	6.9
o	011	25	..	..	1	2	6	3	1	2	2	3	..	..	..	..	..	..	..	..	..	..	..	..	..	..	..	..	..	..	..	..	6.4
i	132	23	..	..	..	1	1	3	5	3	5	2	..	2	..	1	..	..	..	..	..	..	..	..	..	..	..	..	..	..	..	..	5.3
ô	113	16	..	..	..	1	1	2	3	2	..	4	2	..	1	..	..	..	..	..	..	..	..	..	..	..	..	..	..	..	..	..	8.3
h	130	13	..	..	..	1	3	1	1	..	3	2	1	..	1	..	..	..	..	..	..	..	..	..	..	..	..	..	..	..	..	..	7.9
u	021	11	..	..	..	..	..	..	..	1	2	1	1	3	2	..	..	..	..	1	..	..	..	..	..	..	..	..	..	..	..	..	11.5
z	121	10	..	..	..	..	..	..	..	1	2	2	..	2	..	..	1	1	..	..	..	..	..	..	1	..	..	..	..	..	..	..	12.4
b	221	9	..	..	..	..	..	..	1	..	..	1	3	1	3	..	..	..	..	..	..	..	..	..	..	..	..	..	..	..	..	..	11.2
d	241	8	..	..	..	..	..	..	..	..	1	1	2	1	..	2	..	..	..	..	..	..	..	1	..	..	..	..	..	..	..	..	13.0
r	112	6	..	..	..	..	..	..	..	3	..	..	2	..	..	..	..	..	1	..	..	..	..	..	..	..	..	..	..	..	..	..	10.6
x	133	6	..	..	..	..	..	..	1	..	..	..	..	..	1	1	1	..	1	..	..	..	..	..	..	..	..	1	..	..	..	..	15.3
v	151	5	..	..	..	..	..	..	..	..	..	1	1	1	..	..	..	1	1	..	..	..	..	..	..	..	..	..	..	..	..	..	13.2

Classement définitif: $m\ a\ (c\ p)\ s\ f\ (l\ o)\ i\ \delta\ h\ u\ (z\ b)\ d\ r\ x\ v$.

A ces formes, il faut ajouter les suivantes, dont la fréquence absolue est inférieure à 5 et pour lesquelles la notion de rang moyen perd toute signification:

γ	η	α	π	$\varkappa$	ν	ω	l	Δ	ψ	e	(σ	δ)	β	ξ
118	114	1.1.20	122	031	012	377	243	454	470	351	135	117	1.1.10	032

(ϵ	ϱ	λ)	r_1	μ	y	φ	TN	g	F	Y_3	L_3	L_2	Y_1
116	383	445	461	885	141	350	441	5.20.2	7.13.1	481	8.10.5	571	5.19.2

Les formes entre parenthèses sont de même importance.

(*hk*0), (0*kl*) et (*hhl*). La zone des faces (0*kl*) est la même que celle des faces (*h*0*l*), à cause de la symétrie tétragonale holoèdre.

(1) La zone *m f* des faces (*hk*0) contient cinq faces qui ont été figurées: *m f h* ψ φ (tableau 7). Le segment harmonique, avec ces faces aux distances respectives 1, 1/2, 1/3, 3/5, 4/7, indique une *zone simple*. Il a toutefois une anomalie dans le manque de faces aux distances 2/3 et 1/4, anomalie sans grand intérêt vu la rareté des faces ψ et φ. L'importance relative des formes *m*, *f* et *h* est très bien marquée.

(2) La zone des faces (0*kl*) comprend, en ordre d'importance décroissante: *o u* π ν ξ, plus deux faces connues, mais rares: A et X (tableau 7). Le segment arithmétique donne les faces *o* (011), *u* (021), π (031), ξ (032) respectivement aux distances 1, 2, 3, 3/2. Sur le segment harmonique, on trouve ν (012) à la distance 1/2, X (013) à 1/3 et A (023) à 2/3. C'est là une *zone simple* parfaite, avec dominante unitaire *o* (011).

(3) Dans la zone des (*hhl*), on a les faces suivantes: *p t* ϑ *b r* γ η α δ β ϵ λ μ ?N (tableau 8). Sur le segment arithmétique, on a, toujours en ordre d'importance décroissante, des faces aux distances suivantes (*c p*

TABLEAU 7.—DÉVELOPPEMENT DES ZONES SIMPLES

Distance au pôle				Zone des faces 0*kl*				Zone des faces *hk*0				Zone des faces *h*.3*h*.*l*			
I	II	III	IV	I	II	III	IV	I	II	III	IV	I	II	III	IV
1/5												ω135			
1/4												(134)			
1/3				X026				*h*260				$\varkappa$133			
1/2				ν024				*f*240				ζ132			
			4/7								ψ8.14.0				
		3/5								φ6.10.0					
	2/3				A046				(460)						
1				*o*022				*m*220				*s*131			
	3/2				ξ064										
2				π042											
3				ν062											

REMARQUE.—Les formes non observées ont leur symbole entre parenthèses.

TABLEAU 8.—DÉVELOPPEMENT DES ZONES DOUBLES

Distance au pôle			Zone des faces *hhl*			Zone des faces *hkk* ou *hkk*		
I	II	III	I	II	III	I	II	III
1/9			χ119					
	2/16			γ2.2.16				
1/7			δ117					
	2/12			*e*2.2.12				
1/5			ζ115					
	2/8			η228				
1/3			ϑ113			$\varkappa$133		
		3/7						ω377
	2/4			*r*224			π244	
		3/5			α335			(355)
1			*p*111			*p*111		
	4/2			*b*442			$\varkappa$242	
		7/3						
3			β331			*s*131		
		11/3						
	8/2			?N882			ρ282	
5			O551			ν151		
	12/2						Z2.12.2	
7						ω171		

REMARQUES.—Les formes non observées ont leur symbole entre parenthèses. Les faces O(551), ζ(115), χ(119) sont données comme rares dans l'Atlas; de même que les faces Z(2.12.2) et ω(171).

étant pris pour unité): p à 1, t à 3, b à 4/2, O à 5, ?N à 8/2. Sur le segment harmonique, l'ordre est le suivant: ϑ à 1/3, r à 2/4; les autres faces sont trop rares pour mériter d'être prises en considération. On voit clairement l'existence d'une *zone double* avec dominante unitaire simple p (111).

Les tableaux 7 et 8 ont été dressés sur le modèle des tableaux que Donnay (1938b) a employés pour illustrer le développement théorique des zones.

Dans un réseau à base centrée C, sans plans de symétrie avec glissement (Fig. 3), la zone des faces ($hk0$) serait du type *double;* elle devient *simple* par l'effet d'un plan avec glissement a, perpendiculaire à l'axe d'ordre 4. Dans le cas du réseau C, la zone des faces ($0kl$) serait *simple avec dominante déplacée* (021); la dominante, éloignée de (011) par le mode C du réseau, y est ramenée par un plan avec glissement c. Enfin, en position diagonale, la zone des faces (hhl) serait *simple* dans le cas du seul réseau C; c'est un plan avec glissement n qui la transforme en zone *double*. On a donc pour groupe spatial $C4/acn$, avec le rapport d'axes $c:a=0.5372$ (Fig. 4).

D'après les conventions modernes, il convient d'orienter le cristal de façon à le rapporter à la maille la plus petite possible. Dans le cas présent, la maille (à base centrée) est une maille double; il suffit de tourner le cristal de 45° autour de l'axe vertical pour le rapporter à la maille simple. Dans cette nouvelle orientation (Fig. 5), le réseau est primitif et le groupe spatial se note $P4/nnc$. Le rapport d'axes devient $c:a=0.7597$.

Ces résultats sont d'accord avec ceux que fournissent les rayons X (*Strukturbericht*).

AVERTISSEMENT

Jusqu'ici, j'ai employé les lettres de Goldschmidt pour désigner les formes dans l'orientation C (base centrée). Dans le reste du travail, ces lettres désigneront les mêmes formes *dans la nouvelle orientation*, P. La matrice de transformation est la suivante: $C \rightarrow P = \frac{1}{2}\ \frac{1}{2}\ 0/\overline{\frac{1}{2}}\ \frac{1}{2}\ 0/001$. Les nouveaux indices (HKL) figurent à côté des anciens dans le tableau 9.

TABLEAU 9.—TRANSFORMATION D'INDICES

Indices premiers entre eux			Indices multiples	
C (hkl)	P (HKL)	Lettre	C (hkl)	P (HKL)
110	010	m	220	020
010	110	a	020	110
001	001	c	002	002
111	011	p	111	011
131	121	s	131	121
120	130	f	240	130
331	031	t	331	031
011	112	o	022	112
132	122	i	132	122
113	013	ϕ	113	013
130	120	h	260	240
021	111	u	042	222
221	021	b	442	042
121	132	z	242	132
241	131	d	241	131
112	012	r	224	024
133	123	x	133	123
151	231	v	151	231
118	018	γ	2.2.16	0.2.16
114	014	η	228	028
1.1.20	0.1.20	α	2.2.40	0.2.40
122	134	n	244	134
031	332	π	062	332
012	114	ν	024	114
377	257	ω	377	257
243	133	l	243	133
454	198	Δ	8.10.8	198
470	3.11.0	ψ	8.14.0	3.11.0
351	141	e	351	141
135	125	σ	135	125
117	017	δ	117	017
1.1.10	0.1.10	β	2.2.20	0.2.20
032	334	ξ	064	334
116	016	ϵ	2.2.12	0.2.12
383	5.11.6	q	6.16.6	5.11.6
445	045	λ	8.8.10	0.8.10
461	151	r_1	461	151
885	085	μ	16.16.10	0.16.10
141	352	y	282	352
350	140	φ	6.10.0	280
441	041	?N	882	082
5.20.2	15.25.4	g	10.40.4	15.25.4
7.13.1	3.10.1	F	7.13.1	3.10.1
481	261	Y_3	481	261
8.10.5	195	L_3	8.10.5	195
571	161	L_2	571	161
5.19.2	7.12.2	Y_1	5.19.2	7.12.2

TOTAL INDICIEL

Meen (1939) a observé, provenant de la région du Grand Lac des Esclaves, des cristaux ayant jusqu'à un pouce de long, de couleur brun-chocolat légèrement verdâtre et de facies prismatique trapu; chaque spécimen montrant la base bien développée aux deux extrémités. Il signale que C. Gottfried (1930) a déterminé une maille à base centrée. Il montre que le réseau P apporte une simplification notable des in-

dices. Pour 12 formes, le *total indiciel* (Ungemach, 1935) est 50 dans l'orientation *C* et 38 dans l'orientation *P*. Pour les 48 formes figurées de l'espèce, je trouve les totaux indiciels suivants:

(1) avec les indices de Miller premiers entre eux,

dans l'orientation *C*:536,
dans l'orientation *P*:408;

(2) avec les indices multiples, satisfaisant aux critères du groupe spatial,

dans l'orientation *C*:609,
dans l'orientation *P*:507.

PREDICTION DES DIMENSIONS ABSOLUES DE LA MAILLE

La formule de l'idocrase est encore imprécise. *Strukturbericht* (2: 127. 1937) donne comme formule idéale: $Ca_{10}Mg_2Al_4Si_9O_{34}(OH)_4$. La formule trouvée par Meen est en accord avec celle de Machatschki: $X_{18}Y_{26}Z_{36}(O, OH, F)_{152}$ X = Ca(Na, K, Mn); Y = Al, Fe‴, Fe″, Mg, Ti, Zn, Mn; Z = Si.

Avec la formule proposée par *Strukturbericht*, on trouve que *Z*, le nombre de molécules contenues dans la maille est au minimum de 2, en ce sens que la symétrie du groupe spatial peut être satisfaite si $Z=2$.

Si $Z=2$, on obtient pour le volume de la maille *P*:
$V_0=1380.07$ Å^3, et prenant comme densité moyenne 3.4, on a
$a_0=12.20$ Å et $c_0=9.27$ Å.
Si $Z=4$, les résultats sont: $V_0=2760.14$ Å^3,
$a_0=15.37$ Å et $c_0=11.68$ Å.
Les rayons X donnent:
$a_0=15.63$ Å et $c_0=11.83$ Å,
avec rapport d'axes $c_0:a_0=0.757$.

Dans un cas, tel que celui de l'idocrase, où la formule chimique est très compliquée, on ne peut espérer prédire avec certitude les dimensions absolues de la maille.

LOI DE BRAVAIS CLASSIQUE

La loi de Bravais classique donne l'ordre d'importance des formes en partant du réseau, tandis que la loi généralisée con-

Fig. 6.—Listes théoriques d'importance décroissante des formes: (1) Groupe *P4/nnc* (loi général-Isée); (2) Réseau *P*; (3) Réseau *I* (loi de Bravais classique). Lire de bas en haut.

duit à cet ordre en partant du groupe spatial. La Fig. 6 a été construite à l'aide d'un abaque, analogue à celui de Mallard (1879, 1: p. 314), préparé par M. le Professeur Donnay. *P* 4/*nnc* est le groupe trouvé par la loi généralisée; *P* et *I* sont les deux modes possible du réseau. Si l'on ne connaissait que la loi de Bravais classique, l'ordre observé d'importance relative des formes imposerait le réseau *I*.

Sur la Fig. 6, on lira de bas en haut; le nombre qui suivra la forme est le numéro d'ordre observé tiré du tableau 6. Les 18 premières formes de la liste théorique sont, dans le cas du réseau *P*: *m*(1), *c*(3), *a*(2), *p*(3), *u*(12), *h*(11), *b*(13), *s*(5), *r*(16), *o*(7), (221) (non observée), *f*(6), *t*(7), *d*(15), *i*(9), (230) (non observée), *v*(18), (032) (non observée), tandis que, dans le cas du réseau *I*, elles deviennent: *a*(2), *p*(3), *m*(1), *s*(5), *c*(3), *o*(7), *f*(6), *t*(7), *v*(18), *u*(12), *ϑ*(10), *z*(13), *e*(29), *h*(11), *x*(17), *b*(13), *π*(23), (150) (non observée).

On voit que les 8 premières formes de la liste *I*, ont un numéro d'ordre observé plus petit que 10; que les 5e, 6e, 7e formes de *P* ont les numéros 12, 11, 13 et que le n° 5 viendrait après. En effet, la fréquence absolue de *s*(5) (tableau 6) est 28, tandis que les fréquences de *u*, *h*, *b* sont respectivement 11, 13, 9. La forme *s* est donc beaucoup plus importante que *u*, *h*, *b*. Ceci est déjà un argument en faveur du réseau *I*.

Dans les formes subséquentes, le réseau *P* présente une anomalie en ce que la forme (221) qui arrive 11e dans l'ordre théorique, n'a jamais été observée. Or, dans la liste *I*, cette forme, qui doit obéir au critère d'extinction I (somme paire), se trouve rejetée en dehors du tableau, car en devenant (442) elle voit son importance diminuer de beaucoup.

Dans la liste *P*, les 3 premières formes non observées sont les 11e, 16e et 18e de l'ordre théorique, tandis que dans la liste *I* ce sont les 18e, 20e et 22e. L'absence de ces formes dans *I* ne constitue qu'une légère anomalie, puisque leur rang les classe parmi les formes rares. Dans *P*, au contraire, les trois premières formes non observées viennent avant des formes importantes.

Ces observations montrent que la loi de Bravais classique[4] ferait conclure à un réseau *I*.

RESEAU SIMULE

La loi généralisée a conduit au groupe *P*4/*nnc* et la loi de Bravais classique au réseau *I*. Or le groupe *P*4/*nnc* et le réseau *I* ont les mêmes extinctions sauf pour les faces (*hkl*). Le groupe *P*4/*nnc* n'impose à celles-ci aucune restriction, tandis que le réseau *I* exige que la somme des indices soit paire.

On a donc ici un très beau cas de *réseau simulé*. Ce cas est encore plus typique que celui de l'apophyllite (Donnay, 1937) dont le groupe spatial est *P*4/*mnc* et qui simule aussi le réseau *I*.

Le groupe *P*4/*mnc* n'impose aucune condition aux faces (*hkl*) et (*hk*0).

La figure 6 montre que les deux formes (*hkl*) les plus communes sont *d*(131) et *i*(122). Le critère I (somme paire) diminue de beaucoup l'importance de ces formes et les rejette en dehors du tableau, tandis que dans le cas du groupe *P*4/*nnc* elles sont bien à leur place quant à l'importance observée. De plus *d* et *i* sont plus importantes que *v*, première forme (*hkl*) qui apparaisse dans l'ordre théorique du réseau *I*. L'étude statistique, en effet, a montré que *d* et *i* précèdent *v* en ordre d'importance.

Dans les résultats précédents, l'ordre relatif des formes dans chaque zone était bien marqué et a conduit sans difficulté au groupe spatial *P*4/*nnc*. Cependant l'ordre relatif de toutes les formes entre elles, présente plusieurs anomalies qui ont été indiquées.

L'accord entre l'importance théorique

[4] Mallard (1879, 1, p. 315) utilise l'orientation *P* et il a le bon rapport d'axes *c*:*a*=0.760. L'ordre qu'il a observé est le suivant:

Lévy	h^1	*p*	*m*	a^1	b^1	$a^{1/2}$	$b^{1/2}$	b^1	$b^{1/2}$	h^2	h^2	$b^{1/2}$
Miller	010	001	110	011	112	031	122			120	130	111
Gdt.	*m*	*c*	*a*	*p*	*o*	*t*	*i*			*h*	*f*	*u*

Cet ordre diffère un peu de celui du tableau 6, dans lequel *a* précède *c* et *f* vient avant *o*. Le peu de formes observées ne justifie pas la conclusion de Mallard, qui a cru pouvoir en déduire un réseau *P*. Le réseau *I* s'accorderait d'ailleurs mieux que le réseau *P* avec ces données incomplètes.

des formes et leur importance observée est nonobstant meilleur aux termes de la loi généralisée qu'à ceux de la loi classique.

INDICES MOYENS

La loi des indices moyens (Friedel, 1908), basée sur l'influence de la densité réticulaire, permet de prédire le rapport d'axes à partir des indices des formes connues.

Cette loi tire sa justification de la loi de Bravais. Friedel (1908) en appliquant cette loi à une grande quantité de minéraux a montré que les résultats ne sont d'ailleurs qu'approximatifs.

D'après la loi des indices moyens, on devrait avoir, dans le cas d'une espèce cristalline tétragonale,

$$c:a = 2\Sigma l : \Sigma(h+k),$$

avec une approximation d'autant meilleure que le nombre de formes connues est plus grand.

Dans le cas de l'idocrase, j'ai tenu compte des 47 formes figurées dans l'*Atlas*, ainsi que des 46 autres formes observées.

Dans la première orientation, on trouve: (1) avec les indices de Miller premiers entre eux (réseau *P*), $c:a = 0.759$; (2) avec les indices multiples exprimant la loi de Bravais généralisée (groupe $P4/nnc$), $c:a = 0.764$. Dans la même orientation, les indices multiples exprimant la loi de Bravais classique (réseau *I*) conduisent au rapport $c:a = 0.712$. Le rapport calculé est 0.7597.

Dans la deuxième orientation, on trouve: (1) avec les indices premier entre eux (réseau *C*), $c:a = 0.585$; (2) avec les indices multiples exprimant la loi généralisée (groupe $C\ 4/acn$), $c:a = 0.596$. Les indices multiples exprimant la loi de Bravais classique donnent, dans cette orientation (réseau *F*), $c:a = 0.544$. Le rapport calculé est 0.5372.

Tous ces résultats confirment la validité de la loi des indices moyens dans le cas de l'idocrase. On ne peut cependant en tirer aucune conclusion quant à la possibilité de généraliser cette loi en tenant compte de la symétrie du groupe spatial et en utilisant les indices multiples appropriés.

REMERCIEMENTS

Je remercie Monsieur le Professeur J. D. H. Donnay pour les directives qu'il m'a données au cours de la préparation de ce travail et pour le soin qu'il a mis à revoir mon manuscrit. Je dois à l'obligeance de Monsieur le Professeur C. Faessler les cristaux à facies tabulaire de Laurel.

REFERENCES

DONNAY, J. D. H. *Morphologie de l'apophyllite.* Bull. Acad. Roy. Belgique (Cl. des Sc.) (5) **23**: 749–761. 1937.

———. *Crystal morphology of zircon and rutile.* Mém. Soc. Russe de Minér. (2) **67**: 31–46 (en anglais), 47–62 (en russe). 1938a.

———. *Le développement des zones cristallines.* Ann. Soc. Géol. Belgique **61**: B-260–287. 1938b.

———. *Crystal space-groups determined without x-rays* (abstract). Amer. Min. **24**: 184. 1939.

———. *Analyse morphologique de la danburite.* Trans. Soc. Roy. Canada (3), Section IV, **34**: 33–43. 1940.

———. *Morphologie cristalline de la microlite.* Mém. Soc. Roy. Canada (3), Section IV, **35**: 51–56. 1941.

DONNAY, J. D. H., et HARKER, DAVID. *Généralisation de la loi de Bravais.* Compt. Rend. **204**: 274–276. 1937a.

———. *A new law of crystal morphology extending the Law of Bravais.* Amer. Min. **22**: 446–467. 1937b.

———. *Nouvelles tables d'extinctions pour les 230 groupes de recouvrements cristallographiques.* Nat. Can. **67**: 33–69. 1940.

FRIEDEL, G. *Observations sur les caractéristiques moyennes des espèces cristallines.* Bull. Soc. Franç. Min. **31**: 5–40. 1908.

GOLDSCHMIDT, VICTOR. *Atlas der Krystallformen* **4**: Heidelberg. 1918.

GOTTFRIED, C. *Die Mineralien der Adamellogruppe.* Chemie der Erde **5**: 106–112. 1930.

MALLARD, E. *Traité de cristallographie,* **1**: Paris. 1879.

MEEN, V. B. *Vesuvianite from Great Slave Lake region, Canada.* Univ. Toronto Studies, Geol. Ser., **42**: Contrib. Can. Min., 69–74. 1939.

PEACOCK, M. A. *On normal triclinic face-symbols and the harmonic-arithmetic rule.* Amer. Min. **22**: 210. 1936.

TAYLOR, E. D. *The morphology of columbite crystals.* Amer. Min. **25**: 123–138. 1940a.

———. *Stephanite morphology.* Amer. Min. **25**: 327–337. 1940b.

UNGEMACH, H. *Sur certains minéraux sulfatés du Chili.* Bull. Soc. Franç. Minér. **58**: 97–221. 1935.

BIOPHYSICS.—*Effect of nutrient cultures on the reaction of maize seedlings to light.*[1] J. H. KEMPTON, Bureau of Plant Industry.

Following the demonstration that cultures of nutrient salts increased the size of maize seedlings grown in the dark,[2] it became of interest to determine how the cultures affected the reaction of plants to brief periods of illumination. The present paper reports on a single experiment testing this point.

The nutrient culture used was that given by Eaton[3] at double his concentration and modified by increasing KH_2PO_4 by a factor of 10. The control culture was grown with distilled water.

The plantings were made in coarse, crushed quartz in 40 tin ointment cans covered with tin-sealed tubes. Each can, containing 600 grams of oven-dried quartz moistened with 120 cc of solution or distilled water, was planted with 20 seeds of Funk Yellow Dent. Seed weights were recorded for each lot of 20 seeds.

The cans were kept in a dark room where the air temperature ranged from 85° to 86° F. Four days after planting, one-half the cans from each culture were chosen at random and arranged in a circle at such a distance from a 1,000-watt Mazda lamp as to give each can 100 foot-candles illumination. A strong blast of air was blown just under the lamp at about 3 feet above the plants to prevent, so far as possible, a rise in air temperature. The plants were exposed to this illumination for 1 hour, after which they were again enclosed in tin tubes and left in the dark. During the light exposure the air temperature rose 2° F. Twenty-four hours later the experiment was terminated and the seedlings were measured. Lengths were recorded separately for mesocotyls and coleoptiles. No leaves had appeared at this date—five days after planting. These parts, together with the roots and seed residues, were washed free of the coarse quartz and oven dried at 100° C. The several seedling parts were weighed as products of single cans—not as individual plants.

The measures expressed as means of individuals are given in Table 1 and the analyses of variance are shown in Table 2.

The reaction to light was actually and relatively much greater in the plants grown in the salt solution than in those grown in distilled water. This is shown by the length and weight of mesocotyl, as well as in weight of tops (Figs. 1 and 2A; 2B). The roots were not appreciably affected by the culture or by the light exposure given the tops (Fig.

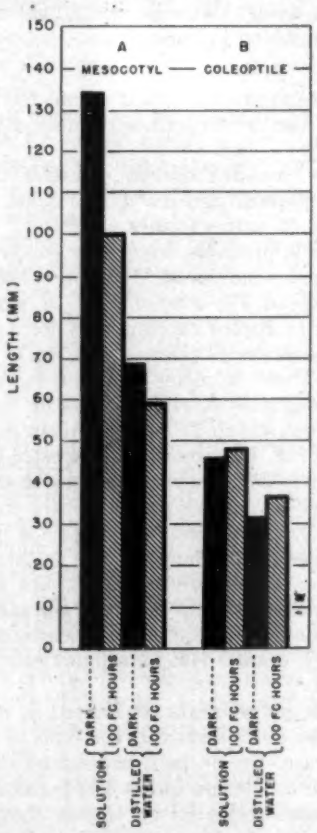

Fig. 1.—Mean length (mm) of mesocotyl (A) and coleoptile (B) of maize seedlings grown in distilled water and in nutrient solution. Solid bars represent seedlings always in the dark, hatched bars seedlings subjected to 100 foot-candle-hours of Mazda light four days after planting.

[1] Received July 31, 1942.
[2] KEMPTON, in press. Journ. Agr. Res.
[3] Journ. Agr. Res. 53: 433–444. September 1936.

2C). The result confirms previous experiments as to the lack of response of roots to culture solutions.[2] The exposure to 100 foot-candle-hours of Mazda increased the length of the coleoptile by a significant amount in the distilled water culture but only slightly in solution (Fig. 1B).

In conformity with the increase in seedling weight, the seed residue shows less material remaining in the seeds planted in the salt solution than in those in distilled water (Fig. 3A). There was little difference between the four treatments in the total amount of dry matter recovered and in the dry matter lost (Figs. 3B and 4B).

The quantity of recovered dry matter translocated is much greater in the seedlings grown in the salt solution than in those grown in distilled water. No such conclusion can be reached with respect to light, as the experiment was not capable of establishing differences in weight of less than 7 per cent. In the plants growing in the salt solutions, 0.06 per cent less dry matter was translocated in the seedlings exposed to 100 foot-candle-hour Mazda and in distilled water the light exposure apparently resulted in a 4 per cent increase in dry matter translocated.

The analyses of variance show that the exposure to 100 foot-candle-hours Mazda illumination affects the weight of the meso-

TABLE 1.—MEASUREMENTS EXPRESSED AS MEANS OF SINGLE SEEDS AND SEEDLING PARTS WHEN GROWN IN THE INDICATED CULTURES IN TOTAL DARKNESS AND IN THE LIGHT SHOWN

Seed or seedling part	Nutrient solution		Distilled water		Standard error of difference
	Dark	100 FC hours Mazda	Dark	100 FC hours Mazda	
	Length (mm)				
Mesocotyl	134.85	100.32	68.80	59.71	3.22
Coleoptile	46.26	48.30	31.67	36.37	1.51
	Weight (g)				
Mesocotyl	.02509	.02047	.01618	.01494	.00075
Tops	.02112	.02503	.01073	.01289	.00077
Roots	.02397	.02464	.02235	.02348	.00077
Seed residue	.1859	.1867	.2073	.1950	.0056
Total dry matter recovered	.2561	.2568	.2566	.2463	.0048
Recovered dry matter translocated	.07018	.07014	.04926	.05131	.00179
Seed planted	.3145	.3159	.3190	.3102	.0056
Lost dry matter	.0584	.0591	.0624	.0639	.0015
Per meter of mesocotyl length	.1861	.2047	.2361	.2505	.0128

TABLE 2.—ANALYSES OF VARIANCE BASED ON MEANS OF 20 SEEDLING GROUPS FOR THE SEED AND SEEDLING PARTS SHOWN

Source of variation	Degrees of freedom	Mean squares										
		Length		Weight								
		Mesocotyl	Coleoptile	Mesocotyl	Tops[1]	Roots	Seed residue	Recovered dry matter	Recovered dry matter translocated	Seed planted	Lost dry matter	Per meter of mesocotyl
Total	39	940.75	58.94	.0000180	.000040	.000004	.000179	.000119	.000116	.000184	.000024	.0015415
Culture	1	28,444.09†	1,757.48†	.0005220†	.001270†	.000020*	.002285†	.000145	.003950†	.000010	.000079	.0229173†
Light	1	4,758.07†	113.44†	.0000860†	.000090†	.000006	.000374	.000229	.000010	.000163	.000005	.0027117
Interaction	1	1,619.23†	17.74	.0000280†	.000010	.000001	.000158	.000111	.000011	.000280	.000038	.0000451
Error	36	51.88	11.39	.0000028	.000003	.000003	.000158	.000115	.000016	.000187	.000022	.0009568

[1] Includes coleoptile, leaves, and stem. * $P<.05$. † $P<.01$.

cotyl and the tops but not the total amount of dry matter translocated. This is illustrated in Fig. 2A and B and Fig. 4A. Evidently even this brief period of low illumination increases the dry matter in the coleoptile and leaves and reduces it in the mesocotyl by approximately an equal amount. The light, therefore, did not increase the speed with which dry matter was moved from the seed but determined its destination by initiating the development of leaves. In a sense, the speed with which

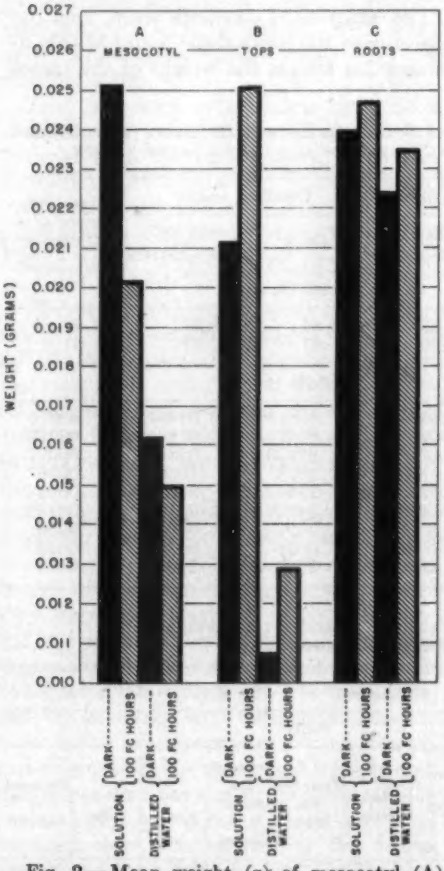

Fig. 2.—Mean weight (g) of mesocotyl (A), tops (B), and roots (C) of maize seedlings grown in distilled water and in nutrient solution. Solid bars represent seedlings always in the dark, hatched bars seedlings subjected to 100 foot-candle-hours of Mazda light four days after planting.

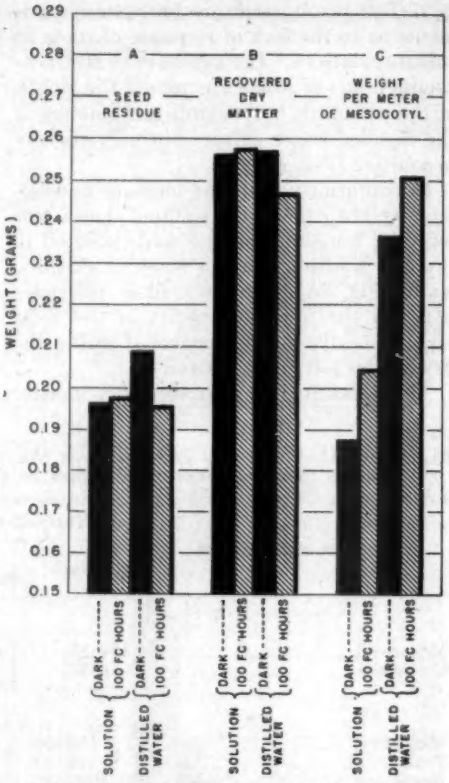

Fig. 3.—Mean weight (g) of seed residue (A), total dry matter recovered (B), and weight per meter of mesocotyl length (C) of maize seedlings grown in the distilled water and in nutrient solution. Solid bars represent seedlings always in the dark, hatched bars seedlings subjected to 100 foot-candle-hours of Mazda light four days after planting.

the solutes travelled up the axis was increased by illumination, since more dry matter was moved into the leaves, but this was accomplished chiefly by stopping the elongation of the mesocotyl, thus reducing the distance from the seed to the leaves. Further, the checking of elongation of the mesocotyl resulted in this organ being heavier per unit length in the lighted series of both cultures, though not significantly so.

Neither the culture nor the illumination affected the quantity of dry matter lost, although the unrecovered dry matter almost equaled the amount translocated.

There is a certain and here unknown loss of weight from diffusion of soluble material into the culture solution and Fig. 4B shows, as would be expected, this factor to be slightly greater in distilled water than in the salt solution. Three other factors contributing to loss of dry matter are in the order of their importance, micro-organisms, oxidation and loss of energy in converting the stored dry matter into soluble forms and finally losses in handling the seedlings. In this experiment this last source of loss must have been inconsequential because the small size of the seedlings made their complete recovery more certain.

The solution used in this experiment is more conducive to leaf development than to mesocotyl elongation, but it exerted a pronounced effect on the sensitivity of the mesocotyl to light. The elongation of the mesocotyl presumably is controlled by growth substances released from the coleoptile, which are inactivated by light. It follows, therefore, that the resistance of these substances to light must be altered by the salts in the solution or else their formation must be reduced. The latter assumption can hardly be urged in view of the very evident stimulation of elongation by the salts in the solution.

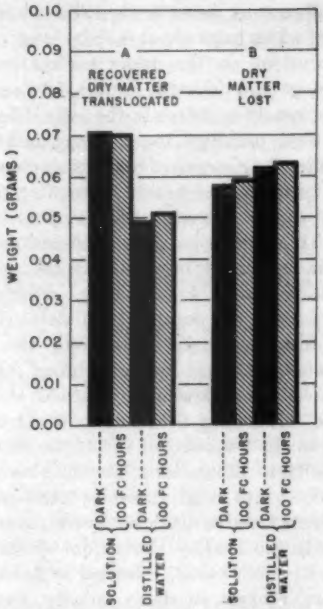

Fig. 4.—Mean weight (g) of the recovered dry matter that had been translocated from the seed to the seedling (A) and dry matter lost (B) of maize seedlings grown in distilled water and in nutrient solution. Solid bars represent seedlings always in the dark, hatched bars seedlings subjected to 100 foot-candle-hours of Mazda light four days after planting.

BOTANY.—*Three new species of Acanthaceae from Mexico.*[1] By E. C. LEONARD, U. S. National Museum. (Communicated by WILLIAM R. MAXON.)

A study of Mexican Acanthaceae in the U. S. National Herbarium and the Dudley Herbarium of Stanford University, in connection with preparing a treatment of the family as it occurs in the Sonoran Desert region, has revealed three new species. These are described herewith. One is from Baja California, another from Veracruz, and the third from the west-central portion of the republic.

Buceragenia ruellioides Leonard, sp. nov.

Herba, caulibus pubescentibus; petioli alati; lamina foliorum oblonga vel late elliptica, breve acuminata vel acuta, basi angustata, parce puberula; flores solitarii vel fasciculati, bracteis foliaceis suffulti; bracteae floriferae lineari-lanceolatae, pubescentes, ciliatae; bracteolae subulatae, puberulae; calyx puberulus, segmentis subulatis, ciliatis; corolla minuta, subregularis, lobis ovatis; stamina inclusa; capsulae glabrae; semina muricata.

Herb; stem simple or probably branched, 40 cm high or more, the pubescence a mixture of minute curved hairs and larger spreading ones up to 1 mm long; petioles up to 3 cm long, winged; leaf blades oblong to broadly elliptic, up to 12 cm long and 5 cm wide, short-acuminate to acute (the tip usually blunt), narrowed at base, the blade gradually long-decurrent, thin, rather veiny, inconspicuously and spar-

[1] Published by permission of the Secretary of the Smithsonian Institution. Received July 16, 1942.

ingly puberulous, beset with a few additional scattered white hairs about 0.5 mm long; cystoliths prevalent on the upper surface but inconspicuous and delicate; flowers 1 to several, sessile or nearly so, borne in the axils of leaflike bracts, these usually 1 to 2 cm long and 0.5 to 1 cm wide, the lowermost bracted clusters subtended by the leaves; bracts subtending the individual flowers linear-lanceolate, 6 to 9 mm long, 1.5 mm wide, sparingly pubescent, ciliate, the costa prominent; bractlets subulate, ciliate, puberulous; calyx 4 mm long, puberulous, deeply parted, the segments subulate, ciliate; corolla tubular, barely 3 mm long, the lobes ovate, about 0.5 mm long and broad, obtuse, the posterior ones sparingly bearded; stamens included, 1 mm long, the staminodes about half as long as the filaments of the fertile stamens; capsules 10 to 12 mm long (the solid basal portion about 5 mm long), glabrous, 2 to 4-seeded; seeds about 2 mm in diameter, brown, muricate.

Type in the Dudley Herbarium of Stanford University, no. 184953, collected at Zacuapan, Veracruz, Mexico, in shady locality, October, 1929, by C. A. Purpus (no. 14083).

This species is well marked and easily distinguished from other members of the genus by its leafy inflorescence. Because of its minute and inconspicuous bracted flower-clusters and a certain resemblance in the leaves, it is possible to mistake it for cleistogamous plants of *Ruellia strepens* L.

Justicia wigginsii Leonard, sp. nov.

Frutex, caulibus pluribus, striatis, albopuberulis, infra glabratis, griseis; petioli breves; lamina foliorum ovata, obovata, vel lanceolata, apice rotundata vel acuta, basi angustata, minute puberula: spicae secundae, laxae, glanduloso-puberulae; bracteae subcucullatae; bracteolae lanceolatae; calycis segmenta puberula, glanduloso-ciliiolata, posticum minutum setaceum, altera lineari-lanceolata; corolla rubra, labio superiore erecto, apice bilobo, inferiore trilobo, patulo, lobis oblongis, rotundatis; stamina exserta; capsulae parce glanduloso-puberulae; semina valde tuberculata et minute papillosa.

Shrubs; branches numerous, striate, closely white-puberulous, the older portions glabrate, gray; petioles slender, up to 5 mm long; leaf blades ovate, obovate, or lanceolate, up to 2 cm long and 1 cm wide, rounded to acute at apex, narrowed at base, inconspicuously puberulous; flowers borne in loose secund spikes, these puberulous, with glandular and eglandular hairs intermixed; bracts in threes, glandular-ciliate, the middle one 2.5 mm long, subcucullate, the lateral ones lanceolate, 3 mm long, about 0.75 mm wide near base; calyx deeply 5-parted, the posterior segment subulate, about 3 mm long, the others linear-lanceolate, about 6 mm long and 1.5 mm wide, rather firm, indistinctly striate-veined, puberulous and glandular-ciliate; corolla up to 3 cm long, red, finely but sparingly pubescent, the tube about 1 cm long, somewhat saccate, the upper lip straight, erect, 2-lobed at apex, the lower lip somewhat spreading, 3-lobed, the lobes oblong, about 7 mm long, rounded at apex, the middle lobe about 4 mm wide at base, the lateral ones about 2 mm wide; stamens about as long as the upper lip, the anther cells unequal, one 2 mm long, the other 2.5 mm long, the lobes spreading at base; capsules 11 mm long, sparingly glandular-puberulous; seeds flattened, 2.5 mm broad, strongly tuberculate, minutely papillose.

Type in the Dudley Herbarium of Stanford University, no. 263987, collected in a rocky wash 27.7 miles south of Pozo Alemán, Baja California, March 4, 1935, by Ira L. Wiggins (no. 7874). A specimen collected by Brandegee from cliffs at Comondu, Baja California, March 21, 1889, without number, is also this species.

Justicia wigginsii is a peculiar plant having the inflorescence of *J. hians* Brandeg. and the corolla of *J. mexicana* Rose, but differing from both in its irregular calyx.

Jacobinia roseana Leonard, sp. nov.

Frutex, caulibus subteretibus, glabris, gracilibus; petioli breves; lamina foliorum ovato-lanceolata vel ovata, acuminata, basi angustata in petiolum decurrens, supra glabra, subtus in axillis venarum parce barbata; flores plures, conferti, axillares; bracteae lineares, hirtellae, plus minusve ciliatae; bracteolae subulatae, minute hirtellae; calyx puberulus, segmentis lanceolatis, acuminatis; corolla rubra labio superiore apice minute bilobo, inferiore trilobo, lobis oblongis, rotundatis; stamina exserta; capsulae glabrae; semina rubra vel fusca, tuberculata.

Shrub up to 1 meter high or more; stems slender, subterete, glabrous or sparingly and minutely pubescent near the nodes; leaf blades ovate-lanceolate to ovate, up to 7 cm long and 3.5 cm wide, acuminate (the tip blunt), narrowed at base and decurrent (petiole up to 1 cm long), entire, glabrous above, beneath sparingly barbate in axils of veins; flowers borne in axillary and terminal clusters, often crowded and numerous; bracts linear, about 1 cm long and 1 mm wide, minutely and sparingly hirtellous, ciliolate, often beset with long scattered marginal hairs up to 1 mm long; bractlets subulate, about 5 mm long, minutely hirtellous; calyx 4–5 mm long, the segments puberulous, lanceolate, 3.5 mm long, 1.5 mm wide, acuminate; corolla scarlet, puberulous without, 2.5 cm long, the tube 5 mm in diameter at mouth, the lips subequal, about 13 mm long, the posterior one minutely 2-lobed at apex, the anterior one 3-cleft nearly to middle, the lobes oblong, rounded; stamens about equaling the upper lip, the anthers 2.5 mm long, the cells parallel, unequally attached to the connective; capsule 1 cm long and 5 mm in diameter, narrowed to a solid stipitate base 5 mm long, glabrous, 4-seeded; seeds reddish brown, slightly flattened, about 2.5 mm broad, tuberculate.

Type in the U. S. National Herbarium, No. 208675, collected at Manzanillo, Colima, Mexico, December 1 to 31, 1890, by Edward Palmer (no. 946). Besides a specimen from the same locality (*Ferris* 6034), the following additional material has been examined:

MICHOACÁN: Coalcomán, *Hinton* 12620, 15845, 16104.

MORELOS: Xochitepec, *Lyonnet* 1173, 1515, 2652.

MEXICO: Temascaltepec, *Hinton* 5190.

The present species is closely allied to *J. mexicana* but differs in its narrow bracts and bractlets, these definitely exceeding the calyx. On the basis of *Palmer* 946 it was described by Dr. J. N. Rose[2] long ago, but no species name was given it by him. The more ample recent material above cited agrees closely.

[2] Contr. U. S. Nat. Herb. 1: 349. 1895.

BOTANY.—*Two zoophagous species of* Acrostalagmus *with multicellular* Desmidiospora*-like chlamydospores.*[1] CHARLES DRECHSLER, Bureau of Plant Industry.

Considered collectively, the fungi that under terrestrial conditions attack actively motile eelworms after the usual manner of parasites, by invading them with germ tubes from affixed or ingested conidia, show more than an ordinary degree of morphological distinctiveness. The zoopagaceous form I described earlier (2) as *Euryancale sacciospora* bears curiously appendaged conidia on lateral branches of bizarre outward shape. In the helicoid modification of their distal portions, as also in the close septation of these portions, and in the production on them, mostly laterally, of plural sessile conidia, the conidiophores of my *Meristacrum asterospermum* (3) embody features thoroughly alien to the more familiar insectivorous members of the Entomophthoraceae. The somewhat similar conidophores of the hyphomycetous parasite I named *Meria coniospora* (4), which in their transverse septation and in their production of conidia on slender sterigmata arising singly from the delimited segments show curious analogy with promycelia of the rusts as well as with the basidia of *Auricularia*, appear to have no parallel among the Mucedinaceae except in *Meria Laricis* Vuillemin [= *Hartigiella Laricis* (Hartig) Lindau], a fungus whose sporulation was held very unusual both by Vuillemin (8) and by Lindau (5). *Harposporium anguillulae* Lohde (6) as set forth by Zopf (9) offers marked individuality in its globose conidiiferous branches and curious sickle-shaped conidia. Globose conidiiferous branches and conidia of peculiar design likewise give distinctive character to the three congeneric parasites which I presented as new species under the binomials *H. helicoides*, *H. oxycoracum*, and *H. diceraeum* (4).

On the other hand no exceptional distinctiveness attaches to the four nematode-destroying parasites I described as *Acrostalagmus bactrosporus*, *A. obovatus*,

[1] Received August 8, 1942.

Cephalosporium balanoides, and *Spicaria coccospora* (4). With respect to the morphology of their conidial apparatus these species show close correspondence with the rather numerous group of entomogenous fungi that in large part have been subsumed under the same genera; the correspondence, indeed, appearing rather clearly presumptive of an intimate taxonomic relationship. Further evidence in favor of such a relationship is supplied by two similar hyphomycetous parasites that have come under my observation, one attacking eelworms, the other attacking rotifers.

The former parasite made its appearance in a maizemeal-agar plate culture that after being occupied by a species of *Pythium* had been further planted with a few pinches of leaf mold gathered in Arlington, Va., on January 7, 1941. A species of *Bunonema* introduced with the forest refuse, and like other representatives of the genus feeding only on the surface of agar plates, had multiplied steadily during the first four weeks to attain a population of approximately 2000 individuals. Scattered specimens were then observed succumbing to fungus infection. Additional animals were found dead on successive days, until by the end of another week all active individuals of the species were exterminated.

Owing to optical difficulties it was not possible to observe the entrance of the fungus into the animal host, or to follow the progress of mycelial invasion. After an infected eelworm had died, however, and been largely expropriated of its globulose degenerating contents, the fully developed assimilative mycelium became plainly visible. In many instances, a single filament, rather closely septate and bearing some few lateral branches, extended the entire length of the animal's body (Fig. 1, A, B), while in other instances two main filaments could be recognized (Fig. 1, C). From this decidedly meager mycelium two or three branches were soon pushed through the host integument to develop externally as colorless fertile hyphae (Fig. 1, A, a; B, a, b). The fertile hyphae that came to project into the air by virtue of an erect or ascending posture, as also the aerial terminations of similar hyphae procumbent in their proximal portions, often bore two, three, or four flask-shaped conidiiferous branches in verticellate arrangement at the distal end of one or more of their constituent segments (Fig. 1, A, b; C, a; D; E; F). Somewhat less often conidiiferous branches were borne singly on aerial portions of fertile hyphae (Fig. 1, C, a; D), while in procumbent portions they almost invariably arose singly and erect to present more nearly the appearance of autonomous conidiophores (Fig. 1, G). Regardless of posture and position, each flask-shaped branch produced at its tip usually from 5 to 15 small, hyaline, irregularly angular conidia (Fig. 1, H), which remained attached in a cohering cluster.

In addition to the conidial apparatus just described the fungus was occasionally found producing knots of yellowish-brown thick-walled cells within the agar culture medium underlying the body of a parasitized nematode. Some of these knots, or chlamydospores, if such they may be called, consisted of only three or four enlarged globose cells, which from their linear arrangement obviously represented distal segments of rather short hyphae that after emerging from the animal's body had directed their growth downward into the subjacent culture medium (Fig. 1, C, b). In the larger specimens three or four cells were likewise often present in a single row, but here they merely formed a stalk on which was borne distally an expanded part composed of 10 to 15 cells in sarciniform arrangement—the whole structure usually having a flattened clavate shape (Fig. 1, B, e). The colored cells of the chlamydospores, unlike the colorless cells of the fertile hyphae, contained numerous small globules of apparently somewhat oily character.

Development of submerged multicellular resting bodies supplementary to the production of hyaline aerial conidia on flask-shaped terminal or lateral branches has not been seen in any material of *Acrostalagmus bactrosporus*, *A. obovatus*, *Cephalosporium balanoides*, or *Spicaria coccospora*. Among the other hyphomycetes that I have observed attacking nematodes after the

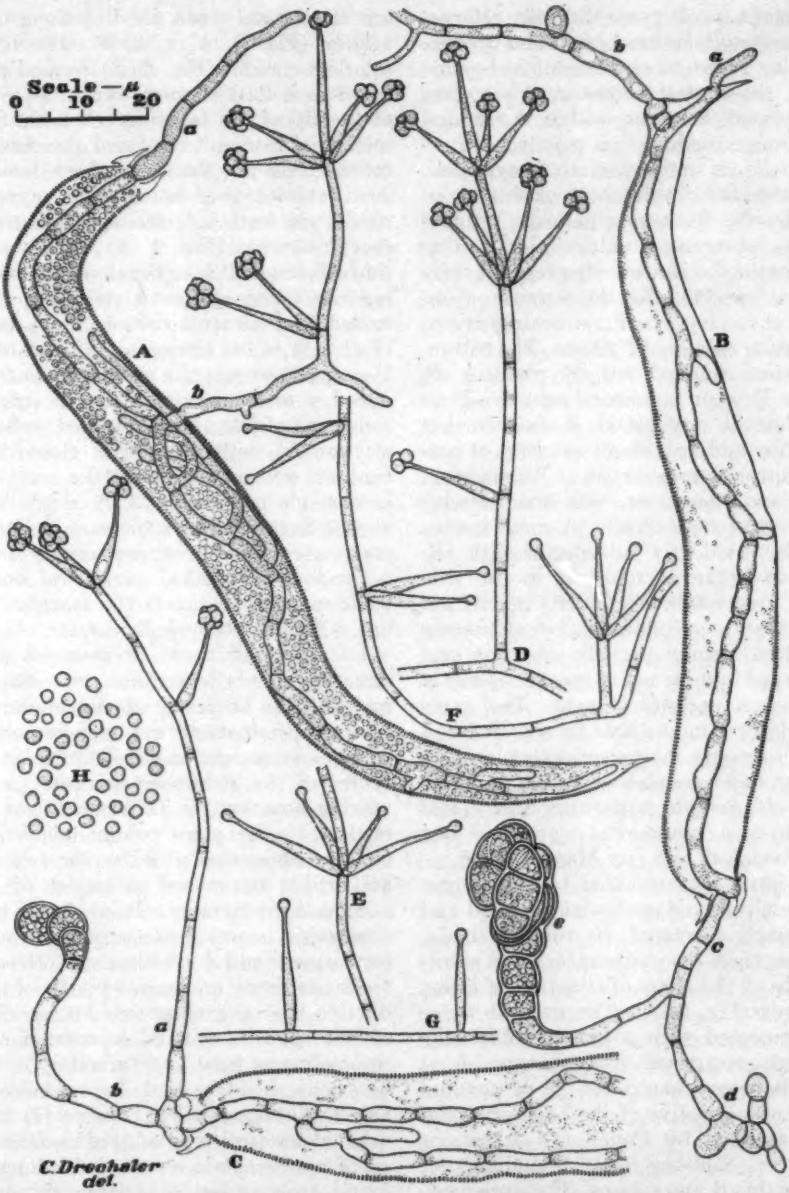

Fig. 1.—*Acrostalagmus goniodes*, drawn to a uniform magnification with the aid of a camera lucida; ×1,000 throughout. *A*, Specimen of *Bunonema* sp. killed by the parasite; from the assimilative mycelium two branches, *a* and *b*, have been put forth externally; *b* has given rise to an erect conidiophore. *B*, Specimen of *Bunonema* sp. killed by fungus and almost depleted of its contents; the assimilative mycelium has put forth three external hyphae, *a*, *b*, *c*; the hypha *c* has given rise to an abortive chlamydospore, *d*, and to a well developed chlamydospore, *e*. *C*, Anterior portion of parasitized *Bunonema* host; from the assimilative mycelium an erect conidiophore, *a*, has grown out, together with a submerged branch, *b*, on which a small chlamydospore has been formed. *D*, An erect conidiophore. *E*, *F*, Portions of ascending conidiophores. *G*, Prostrate hypha bearing two erect conidiiferous branches. *H*, Conidia, showing variations in size and shape.

usual manner of parasites only *Harposporium anguillulae* has been found producing resting bodies to supplement its hyaline conidia, the resting bodies in this species being formed, however, within the animal host through modification mostly of intercalary cells in the assimilative mycelium. Apart from the development of chlamydospores by the *Bunonema* parasite, production of submerged multicellular resting bodies was noted in a culture prepared early in December, 1932, for the purpose of obtaining chytridiaceous fungi destructive to root-rotting species of *Pythium*. The culture in question was started by planting *P. ultimum* Trow on maizemeal-agar in a Petri dish. Several days later it was further planted by adding a small quantity of potting soil from a greenhouse in Washington, D. C., and, moreover, was flooded with about 1 cc of sterile water. A small species of rotifer, evidently introduced with the soil, soon began to multiply in the thin layer of free water. At first its population increased without hindrance, but after some weeks had elapsed periodic examinations never failed to show many specimens newly killed by a parasitic fungus. The same fungus later came to light as a parasite of small rotifers in a maizemeal-agar plate culture that had been planted with a decaying watercress (*Rorippa nasturtium* Rusby) leaf taken from a commercial watercress bed near Woodstock, Va., on May 13, 1938.

Individual rotifers killed by the fungus were usually found each with its head and tail strongly retracted; its rounded body, often less than 75μ in diameter, then showing little of the shape distinctive of living specimens (Fig. 2, A). The fleshy interior was permeated with a hyaline branching mycelium, composed of hyphae which at intervals were constricted in a manner somewhat suggestive of the haustorial filaments ascribed by Couch (1) to various species of *Septobasidium*, including, for example, his *S. purpureum*. The upper surface of the dead animal was usually overgrown abundantly with erect or ascending hyaline conidiophores whose axial filaments bore flask-shaped conidiiferous branches, mostly in whorls of three, immediately below the several septa dividing them transversely (Fig. 2, A, a, b, c). The oblong colorless conidia (Fig. 2, B) formed at the tip of each flask-shaped branch, as well as at the tip of the tapering cell terminating each axial filament, remained attached in a cohering cluster. On the under side of the dead animal the assimilative mycelium would put forth into the agar substratum short filaments (Fig. 2, A, d) that sometimes concluded their development by giving rise terminally to a yellowish, thick-walled, globose structure either continuous (Fig. 2, A, e) or uniseptate (Fig. 2, A, f). Usually, however, the short filaments produced a much more distinctive structure consisting of 8 to 15 thick-walled, yellowish or brownish cells, filled with globuliferous contents and arranged, for the most part, in a single layer (Fig. 2, A, g–n). When viewed flatwise these structures in some instances presented a rather smoothly circular or smoothly elliptical peripheral outline, while in other instances the marginal outline was characteristically lobate.

Despite their more pronounced differentiation it is believed that the submerged multicellular bodies produced abundantly by the rotifer parasite are truly homologous with the submerged multicellular chlamydospores of the *Bunonema* parasite. A convincing homology is likewise evident with respect to the more commonplace aerial conidial apparatus whereby the two fungi are readily recognized as species of *Acrostalagmus* presumably related closely to the congeneric nematode-destroying forms, *A. bactrosporus* and *A. obovatus*, even though in the latter forms no accessory type of reproduction has been observed. An association of two types of asexual reproduction corresponding at least approximately to those here concerned was made known more than half a century ago by Thaxter (7) in the original descriptive account of his *Desmidiospora myrmecophila*, a remarkable fungus he found growing out of a large ant on the under side of a rotting log in Connecticut. The hyaline septate mycelium of this entomogenous form was set forth as giving rise at the apex of subulate basally inflated basidia to hyaline subfusiform microconidia

12μ long and 2 to 2.5μ wide. Since the branches that Thaxter designated as basidia in accordance with an older usage are clearly equivalent to the phialides of more recent authors, the conidia produced on them offer obvious homology with the aerial conidia of both the *Bunonema* parasite and the rotifer parasite. Aside from the hyaline microconidia, Thaxter attributed to *D. myrmecophia* the production of curious macroconidia—terminal, flat, short-stalked, multicellular, thick-walled, reddish-brown or fawn-colored bodies, dichotomously lobed several times in succession, 12 to 14μ thick, and measuring 68μ (maximum 90μ) presumably along the median axis and 80μ (maximum 100μ) in the greater dimension transverse to this axis. From Thaxter's description and illustration it is evident that these macroconidia strikingly resemble the resting spores of the rotifer parasite in many respects, as, for example, in their terminal origin on rather short hyphal branches, in their brown coloration, in their unusual dimensional proportions, and in the flat, mostly uniplanar arrangement of their numerous thick-walled component cells. Differences of detail are, to be sure, present in the much greater size and much more pronounced lobation of the macroconidia ascribed to *D. myrmecophila*.

In considering the essential nature of the multicellular resting spores produced by the rotifer parasite it seems significant that although the animal host of this fungus has nearly always been found succumbing on the surface of agar plate cultures, the spores in question were always formed under the surface of the agar medium, while the associated reproductive apparatus referable to *Acrostalagmus* was always extended into the air. In view of these circumstances the multicellular spores must be regarded as having developed in submerged positions from normal preference rather than from constraint. Despite their distinctive morphology they would appear, therefore, to represent chlamydospores rather than conidia, and may appropriately be reckoned in the same category with the similarly yellowish or brownish, thick-walled, globuliferous chlamydospores of *Harposporium anguillulae* and *Arthrobotrys oligospora* Fres. If analogy is not misleading, the remarkable macroconidia of *Desmidiospora myrmecophila* may likewise be more nearly equivalent to chlamydospores than to true conidia. Since much porous absorbent material is often found on the under side of rotting logs, a habitat like that of Thaxter's fungus might during dry periods permit aerial conidia to be formed in positions where during wet spells opportunity is afforded for the production of submerged reproductive bodies.

It is not evident at present that in the group of zoophagous fungi here concerned the production of chlamydospores, even of very distinctive chlamydospores, can be interpreted as an indication of taxonomic separateness. Accordingly the *Bunonema* parasite and the rotifer parasite are described as new members of the genus *Acrostalagmus*.

Acrostalagmus goniodes,[2] sp. nov.

Mycelium nutritum hyalinum, parve ramosum, septatum, intra vermiculos nematoideos viventes evolutum, ex hyphis filiformibus 1.5-3μ crassis constans. Hyphae fertiles extra animal emortuum evolutae, incoloratae, repentes vel ascendentes vel erectae, axe simplices vel parvulum ramosae, vulgo 50–500μ longae, 1.2–2.5μ crassae, in cellulis 7–18μ longis consistentes, quarum quaedam 1–4 ramulos conidiferos (phialas) ferunt; ramulis conidiferis saepe 2–4 verticellatis, lageniformibus, 10–20μ longis, basi 1.2–2.3μ crassis, quoque sursum in sterigma .5μ crassum abeunte et ex apice ejusdem 5–15 conidia deinceps gerente; conidiis cohaerentibus, hyalinis, rotunde polygoniis, plerumque 1.3–2.1μ diam. Chlamydosporae in materia subjacenti oriundae, ex hyphis immersis leniter latescentes, flavidae vel fulvae, parte ulteriore sarciniformes, omnino 12–30μ longae, 6–15μ latae, 3–18 cellulis constantes.

Vermiculos nematoideos speciei Bunonematis enecans habitat in humo silvestri in Arlington, Virginia.

Assimilative mycelium hyaline, somewhat branched, septate, growing within living

[2] γωνιώδης, angular, having reference to the shape of the conidia.

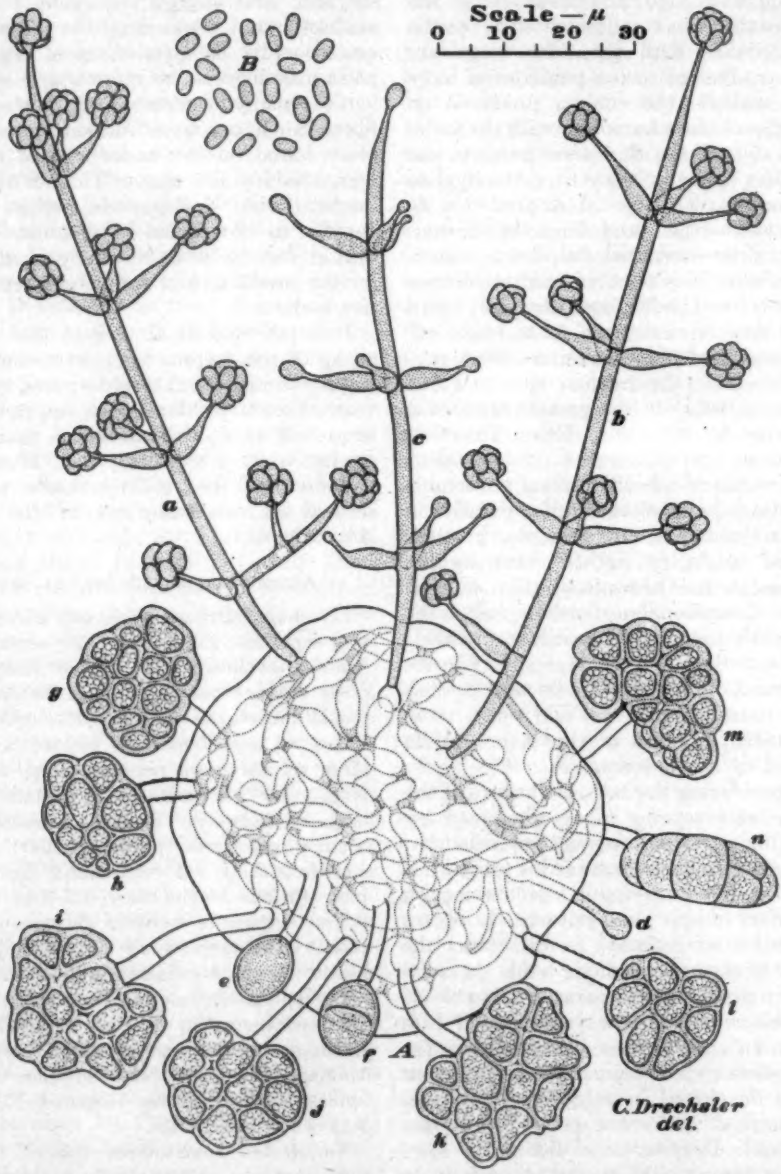

Fig. 2.—*Acrostalagmus tagenophorus*, drawn to a uniform magnification with the aid of a camera lucida; ×1,000 throughout. *A*, Specimen of rotifer killed by the fungus. Three conidiophores, *a*, *b*, *c*, have been extended into the air; *a* and *b* are shown with conidial clusters attached, whereas *c* is shown in denuded condition. Into the underlying material have been extended eleven outgrowths, namely: a young hypha, *d;* two hyphae bearing poorly developed chlamydospores, *e*, *f;* eight hyphae bearing well developed chlamydospores, *g–n*, of which seven, *g–m*, are shown flatwise, whereas one, *n*, is shown edgewise. *B*, Conidia, showing variations in size and shape.

nematodes, and consisting of filamentous hyphae 1.5 to 3μ wide. Conidiophorous hyphae formed outside of the dead animal host, creeping or ascending or erect, colorless, their axial filaments simple or sparingly ramified, commonly 50 to 500μ long, 1.2 to 2.5μ wide, and consisting of segments 7 to 18μ long, of which some bear 1 to 4 conidiiferous branches (phialides); conidiiferous branches often arranged verticellately, flask-shaped, 10 to 20μ long, 1.2 to 2.3μ wide at the base, each tapering distally into a sterigma .5μ wide whereon 5 to 15 conidia are formed one after another to cohere in a head; conidia colorless, rounded polyhedral, mostly 1.3 to 2.1μ in diameter. Chlamydospores formed in the material underlying animal host, each borne terminally on a submerged hypha, its stalk-like proximal part widening gradually into the sarciniform distal part, yellowish or yellowish brown, altogether usually 12 to 30μ long, 6 to 15μ wide, and composed of 3 to 18 thick-walled cells.

Destroying nematodes belonging to a species of *Bunonema* it occurs in leaf mold in Arlington, Va.

Acrostalagmus tagenophorus,[3] sp. nov.

Mycelium nutritum hyalinum, ramosum, septatum, intra viventia animalcula rotifera evolutum; hyphis hic illic constrictis, 1–4μ crassis. Hyphae fertiles extra animal emortuum evolutae, erectae vel ascendentes, incoloratae, axe simplices vel parce ramosae, vulgo 50–250μ longae, magnam partem 1.8–2.5μ crassae, in cellulis plerumque 15–30μ longis constantes quae vulgo 3 (rarius 1 vel 2) ramulos conidiferos (phialas) verticellatos sursum ferunt; ramulis conidiferis lageniformibus, plerumque 10–15μ longis, basi 2.5–3.5μ crassis, sursum in sterigma .5μ crassum abeuntibus, 5–15 conidia deinceps gerentibus; conidiis hyalinis, ellipsoideis vel rotunde oblongis, plerumque 3.5–4μ longis, 2–2.5μ crassis. Chlamydosporae in materia ambienti vel subjacenti immersae, ex hyphis fumadis 5–25μ longis 2–3μ crassis ortae, terminales, fulvae vel olivaceae, applanatae, subdisciformes vel margine aliquid lobosae, vulgo ex 8–15 cellulis constantes, plerumque medio 15–20μ longae, 18–30μ latae, 8–10μ crassae.

Animalia rotifera necans habitat in humo pingui in Washington, D. C., et in foliis *Rorippae nasturtii* putrescentibus prope Woodstock, Va.

Vegetative mycelium colorless, branched, septate, developing within living rotifers, consisting of hyphae 1 to 4μ wide, which here and there are rather markedly constricted. Conidiophores rising erect or ascending from the dead animal host, colorless, their axial filaments simple or sparingly branched, commonly 50 to 250μ long, mostly 1.8 to 2.5μ wide, composed of segments usually 15 to 30μ long which at the distal end commonly bear 3 (less often 1 or 2) conidiiferous branches (phialides) in verticellate arrangement; conidiiferous branches flask-shaped, mostly 10 to 15μ long, 2.5 to 3.5μ wide at the base, terminating in a sterigma .5μ wide, on which 5 to 15 conidia are formed one after another to collect in a cohering head; conidia colorless, prolate ellipsoidal or rounded oblong, mostly 3.5 to 4μ long and 2 to 2.5μ wide. Chlamydospores formed terminally on smoky hyphae often 5 to 25μ long and 2 to 3μ wide, in positions under the surface of the material surrounding or underlying the dead animal host, flat disc-shaped or often with somewhat lobate margin, commonly consisting of 8 to 15 thick-walled cells, along the median axis measuring 15 to 20μ, in the greater dimension transverse to this axis measuring 18 to 30μ, in thickness measuring 8 to 10μ.

Destroying rotifers in rich soil in Washington, D. C., and in decaying leaves of *Rorippa nasturtium* near Woodstock, Va.

[3] τάγηνον, pan for frying, having reference to the shape and attachment of the chlamydospores; and φορέω, to bear.

LITERATURE CITED

1. Couch, J. N. *The genus* Septobasidium: 480 pp. Chapel Hill, N. C. 1938.
2. Drechsler, C. *Five new zoopagaceae destructive to rhizopods and nematodes.* Mycologia **31**: 388–415. 1939.
3. ———. *Three fungi destructive to free-living terricolous nematodes.* Journ. Washington Acad. Sci. **30**: 240–254. 1940.
4. ———. *Some hyphomycetes parasitic on free-living terricolous nematodes.* Phytopathology **31**: 773–802. 1941.
5. Lindau, G. *Die Pilze Deutschlands, Oesterreichs und der Schweiz. VIII. Abteilung: Fungi imperfecti: Hyphomycetes* (erste Hälfte). In Rabenhorst, L., *Kryptogamen-Flora*, ed. 2, Bd. 1, Abt. **8**: 852 pp. Leipzig, 1904–1907.
6. Lohde, G. *Ueber einige neue parasitische Pilze.* Tagebl. Versamml. deut. Naturf. Aertze **47**: 203–206. 1874.

7. THAXTER, R. *On certain new or perculiar North American Hyphomycetes. II.* Helicocephalum, Gonatorrhodiella, Desmidiospora *nov. genera and* Everhartia lignatilis *n. sp.* Bot. Gaz. 16: 201–205. pl. 19. 1891.

8. VUILLEMIN, P. *Les Hyposlomacees nouvelle famille de champignons parasites.* Bull. Soc. Sci. Nancy (2) 14: 15–67. 1896.

9. ZOPF, W. *Die Pilze.* In Schenk, A., *Handbuch der Botanik* 4: 271–781. Breslau. 1890.

ZOOLOGY.—*Some new land shells from Costa Rica and Panama.*[1] HARALD A. REHDER, U. S. National Museum.

The United States National Museum has received from time to time interesting collections of mollusks from Prof. Manuel Valerio, of San José, Costa Rica. Among these sendings several new species of land shells have turned up, which are herewith described. Similarly, the Museum has received a small but valuable collection of land shells from the Province of Chiriquí, Republic of Panama, from Mrs. Robert Adams Terry, among which are two forms that are diagnosed in this paper.

Helicina terryae, n. sp.
Figure 16

Shell small, subglobose, conic, thin but solid. Spire flesh colored, last whorl pale yellow; sculpture when fresh of irregular, oblique, and subspiral grooves on a surface smooth except for obscure growth wrinkles. When worn the shell appears to be sculptured with fine, crowded, wavy riblets or wrinkles, which in fresh shells of this and other species are seen to be part of the shell structure, visible through the periostracal layer. Whorls 4¼, only very slightly convex, suture finely impressed. Aperture oblique, broadly semicircular. Lip thickened, strongly reflexed, broadest in the peripheral region. Columella area thickened, finely granulose, the granulation extending more obscurely over the thin callus. No tooth at the base of the columella.

The type, U.S.N.M. no. 539026, measures: Height, 8.2 mm; diameter, 9.8 mm, and was collected in Chiriquí Province, Republic of Panama.

This little shell is named for the discoverer, Mrs. Robert Adams Terry. It resembles *H. tenuis* but is slightly more depressed and broader, with a broader aperture. The color is also quite distinctive.

Succinea haustrellum, n. sp.
Figure 19

Shell broadly ovate, thin, pale straw yellow in color. Whorls 3, weakly convex, last one very large; suture impressed; sculpture consisting of axial growth wrinkles. Aperture ovate, patulous, columella forms a straight line with the parietal wall.

The type, U.S.N.M. no. 536013, was collected at Pedernal, Guanacaste Province, Costa Rica, at an altitude of 200 meters. It measures: Height, 13.1 mm; breadth, 8 mm.

A smaller paratype, U.S.N.M. no. 536014, is present, as well as two specimens, U.S.N.M. no. 536012, from San José, Costa Rica.

This species differs from the other Central American Succineas in having a shorter spire and larger aperture. The type has the edge of the outer lip somewhat broken.

Spiraxis (Rectaxis) paulisculpta, n. sp.
Figure 18

Shell small, cylindric-turrite, glassy white to pale corneous, translucent, smooth, except for obscure irregular growth wrinkles. Whorls 8+, weakly convex, with a moderately deep, slightly overriding suture. Nuclear whorls not clearly demarcated from postnuclear whorls. First 2¼ nuclear whorls smooth, remaining whorls very gradually widening, sculptured with irregular growth wrinkles. Aperture ovate-lanceolate. Outer lip thin, simple, slightly arcuate, almost vertical; columella straight, slightly oblique.

The type, U.S.N.M. no. 536016, measures: Height, 4 mm; diameter, 1.2 mm, and was collected at Santa María, San José Province, Costa Rica, at an altitude of 1,550 meters. U.S.N.M. no. 536017 contains 10 specimens from the same locality.

This species differs from all the mainland species of *Spiraxis* that I have noted by the weak development of sculpture on the whorls.

[1] Published by permission of the Secretary of the Smithsonian Institution. Received July 31, 1942.

Streptostyla (Streptostyla) valerioi, n. sp.

Figure 17

Shell cylindric-ovate, golden-yellow when fresh, smooth except for very fine irregular growth wrinkles. Nuclear whorls 2¼, rounded, separated by a very fine impressed suture. Postnuclear whorls 4, very slightly convex with an irregular, threadlike subsutural white

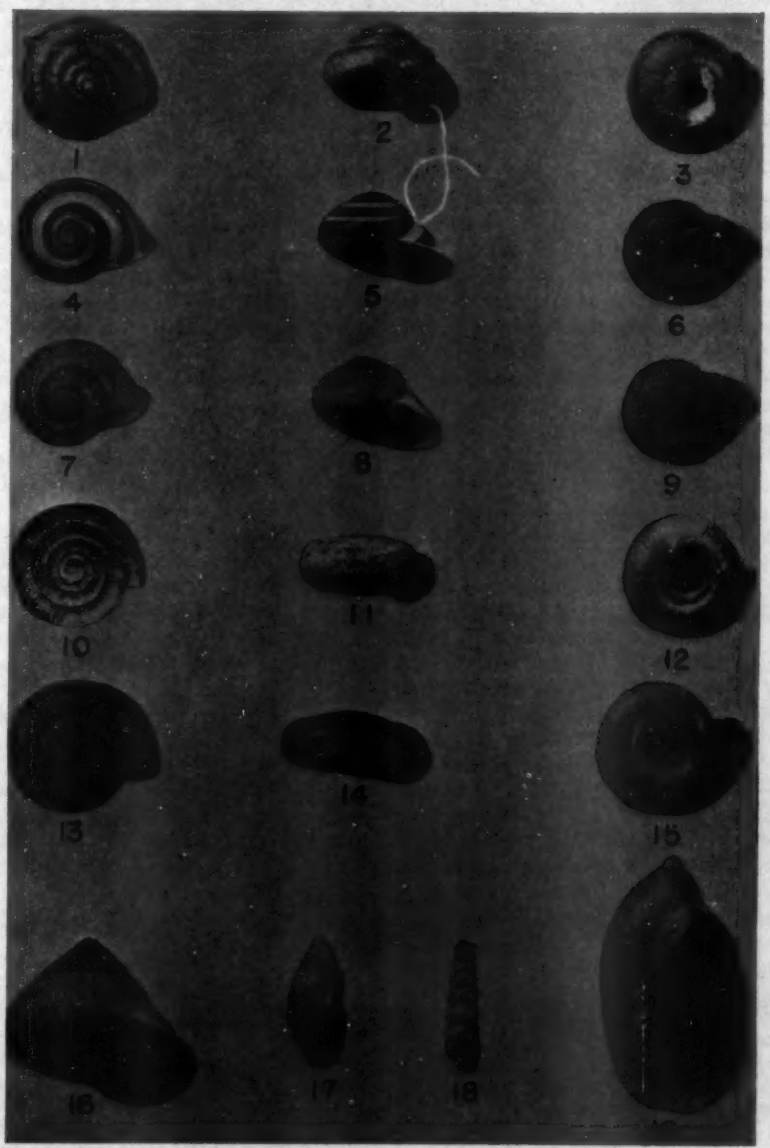

Figs. 1–19.—Land mollusks from Costa Rica and Panama. 1–3, *Thysanophora costaricensis*, n. sp.; 4–6, *Leptarionta venusta venusta* Gude; 7–9, *Leptarionta venusta albata*, n. subsp.; 10–12, *Rotadiscus pilsbryi*, n. sp.; 13–15, *Systrophia* (*Systrophiella*) *costaricana*, n. sp.; 16, *Helicina terryae*, n. sp.; 17, *Streptostyla* (*Streptostyla*) *valerioi*, n. sp.; 18, *Spiraxis* (*Rectaxis*) *pauliscupta*, n. sp.; 19, *Succinea haustrellum*, n. sp.

band; last whorl subcylindric; suture rather irregular, very shallow. Aperture lanceolate, slightly less than half the length of the whole shell; outer lip arched forward in the middle. Columella strongly turrite.

The type, U.S.N.M. no. 536020, measures: Height, 20.2 mm; diameter, 9.1 mm; length of aperture, 10.5 mm, and comes from Cervantes, Cartago Province, Costa Rica, 1,480 meters.

U.S.N.M. no. 536021 contains a paratype from the same locality. Professor Valerio also sent two specimens from Tablazo, San José Province, Costa Rica (U.S.N.M. no. 536022), collected at 1,800 meters, and two specimens from La Verbena, San José Province, Costa Rica (U.S.N.M. no. 536024), collected at 1,000 meters. A specimen collected by Dr. W. M. Mann at Navarro, Cartago Province, Costa Rica (no. 365678) appears to belong here also.

S. valerioi differs from other Streptostylas of Panama and Costa Rica in its cylindric shape and short aperture.

Rotadiscus pilsbryi, n. sp.
Figures 10–12

Shell very small, discoid, horn colored, rather closely coiled, with flattened spire. The nucleus, of 1¼ whorls, is smooth, glassy, while the remaining 3 whorls are sculptured with more or less equidistant axial ribs which have finer axial threads between them. Suture rather deep. Umbilicus rather broad, measuring about one-third of the diameter of the shell. Aperture crescentic; peristome simple, thin.

The type, U.S.N.M. no. 536018, measures: Height, 1 mm; greater diameter, 2.1 mm, and comes from Santa María, San José Province, Costa Rica, at an altitude of 1,550 meters.

U.S.N.M. no. 536019 contains four specimens from the same place.

From *Rotadiscus hermanni* Pfeiffer, Veracruz, Mexico, this species differs in being slightly larger and in having coarser sculpture, riblets being larger and more distantly spaced.

Thysanophora costaricensis, n. sp.
Figures 1–3

Shell of medium size for the genus, moderately depressed, horn colored. Whorls 4¼, convex, somewhat flattened below the deeply impressed suture, last whorl descending slightly. Nuclear whorls 1¼, of which the first ¾ whorl is smooth, the next whorl marked by evenly separated, retractive riblets. Postnuclear whorls marked by rather coarse, retractive, cuticular riblets crossing the strong axial growth wrinkles. These retractive riblets are irregular and often interrupted, with comparatively wide interspaces. The umbilicus is deep and moderately large, contained about 4 times in the diameter of the shell; the walls of the umbilicus are sculptured with granules axially arranged along the growth lines. Aperture almost circular; lip simple, thin.

The type, U.S.N.M. no. 536009, measures: Height, 3.0 mm; diameter, 4.1 mm, and was collected at La Caja, near San José, San José Province, Costa Rica, at 1,000 meters.

Six specimens from the same locality are contained in U.S.N.M. no. 536010 and several specimens were collected at San José, Costa Rica, U.S.N.M. no. 536011.

This species resembles in shape *T. balboa* Pilsbry from Panama, which, however, is larger and has finer retractive riblets.

Systrophia (Systrophiella) costaricana, n. sp.
Figures 13–15

Shell small, subdiscoid, spire slightly elevated, periphery rounded, thin, pale straw-yellow. Nuclear whorls almost 2, convex, smooth; postnuclear whorls 2¼, convex, smooth except for growth wrinkles; suture moderately deep. Umbilicus moderately narrow, measures less than one-third of the diameter of the shell. Aperture broadly lunate; peristome thin, simple.

The type, U.S.N.M. no. 536023, measures: Height, 3.7 mm; greater diameter, 7.7 mm, and was collected at Coto on the Golfo Dulce, Puntarenas Province, Costa Rica, at an altitude of 20 meters.

This species is geographically close to *S. (S.) zeteki* Pilsbry, from Panama, but is smaller, comparatively higher, with a more elevated spire and a smaller umbilicus. It likewise lacks the spiral striae of that species.

Leptarionta venusta albata, n. subsp.
Figures 7–9

Like the typical form but completely white, except for a small chestnut area around the umbilical region; apex slightly greenish yellow.

The type, U.S.N.M. no. 536030, measures: Height, 14.2 mm, diameter, 20.4 mm, and was collected by Mrs. Terry in Chiriquí Province, Panama. Two other specimens from the same source are under U.S.N.M. no. 536031.

A specimen with the typical coloration, also collected by Mrs. Terry in Chiriquí, is depicted in Figs. 4–6.